Journal of Mechanical Engineering and Manufacturing
https://www.sciltp.com/journals/jmem

Review

Friction Stir Welding of Dissimilar Materials: A Comprehensive Study on Joining Stainless Steel to Ni, Ti, and NiTi Alloys

Naiara P. V. Sebbe [1,2,*], Andresa Baptista [1,3], Gustavo Pinto [1,3] and Fábio Fernandes [4]

[1] CIDEM, ISEP, Polytechnic of Porto, 4249-015 Porto, Portugal
[2] FEUP—Faculty of Engineering, University of Porto, 4200-465 Porto, Portugal
[3] LAETA-INEGI, Associate Laboratory for Energy, Transports and Aerospace, 4200-465 Porto, Portugal
[4] TEMA, Department of Mechanical Engineering, University of Aveiro, 3810-193 Aveiro, Portugal
* Correspondence: napvs@isep.ipp.pt; Tel.: +351-22-83-40-500

How To Cite: Sebbe, N.P.V.; Baptista, A.; Pinto, G.; et al. Friction Stir Welding of Dissimilar Materials: A Comprehensive Study on Joining Stainless Steel to Ni, Ti, and NiTi Alloys. *Journal of Mechanical Engineering and Manufacturing* **2026**, *2*(2), 14. https://doi.org/10.53941/jmem.2026.100014

Received: 20 February 2026
Revised: 9 March 2026
Accepted: 23 March 2026
Published: 14 April 2026

Abstract: Friction Stir Welding (FSW) has emerged as a transformative solid-state joining technology, overcoming the metallurgical hurdles inherent in conventional fusion welding. By operating below the melting point of the base materials, FSW suppresses solidification defects, minimizes thermal distortion, and prevents elemental volatilization, critical factors for high-performance alloys. This study provides a comprehensive investigation into the FSW of stainless steel joined to dissimilar non-ferrous systems: Nickel (Ni), Titanium (Ti), and Nickel-Titanium (NiTi) shape memory alloys. The research evaluates the microstructural evolution and the diffusion-controlled kinetics, grain refinement through dynamic recrystallization, and the kinetics of interfacial intermetallic compounds (IMCs). A strategic assessment using SWOT analysis is employed for each material system to identify technical strengths, such as the preservation of the superelastic plateau in NiTi joints and the achievement of tensile strengths exceeding 1100 MPa through post-welding treatments. Furthermore, the study clarifies the phenomenological conditions for the 1 μm Fe-Ti reaction layer threshold, establishing its applicability for thin-gauge structural integrity. By synthesizing current advancements in tool geometry and thermal management, this work highlights the potential of FSW for advanced multi-material applications in the aerospace and biomedical sectors, providing a roadmap for overcoming the rheological and chemical challenges of joining reactive, high-melting-point alloys within contemporary manufacturing frameworks.

Keywords: solid-state joining; interfacial kinetics; dynamic recrystallization; shape memory effect; thermomechanical processing; joint integrity

1. Introduction

Since its inception in 1991, Friction Stir Welding (FSW) has evolved from a specialized niche for aluminum alloys into a transformative solid-state joining paradigm [1,2]. By maintaining the processing temperature below the liquidus line, FSW fundamentally circumvents the deleterious phenomena associated with fusion welding, such as solidification cracking, excessive shrinkage, and the formation of expansive heat-affected zones (HAZ) [3]. While the joining of light alloys (Al, Mg) is well-matured, the transition to high-melting-point materials—specifically stainless steels—represents a frontier characterized by extreme thermo-mechanical gradients and accelerated tool degradation [4,5].

Despite these advantages, the application of FSW to high-melting-point materials remains a complex challenge. While research into aluminum alloys is well-matured [5,6], and significant progress has been made in magnesium [7], copper [8] and titanium [9], the welding of steel types, most notably carbon and stainless steels, remains a complex challenge. The welding tool is often subject to premature failure and a limited-service life due to the high hardness and elevated flow stresses of these materials, which impose severe thermal and mechanical loads on the tool compared to the processing of softer alloys.

In this context, recent investigations have focused on the degradation mechanisms of high-performance tools, such as Tungsten Carbide (WC). For instance, Siddiquee and Pandey [10] using Taguchi's experimental design have demonstrated that tool wear and plastic deformation are highly sensitive to shoulder diameter and the rotation-to-traverse ratio. Specifically, wear at the pin root and bottom face has been attributed to a combination of diffusion and attrition mechanisms, while excessive thermal input can lead to significant tool bulging and alterations in the pin's cone angle. These geometric instabilities not only increase processing costs but also compromise the volumetric integrity of the resulting weld. Beyond these macroscopic challenges, the microstructural refinement in stainless steel FSW is governed by complex crystallographic transformations. In this regard, Mironov et al. [11] investigated the structural response of superaustenitic stainless steel, noting that in materials with low stacking fault energy (SFE), the development of the stir zone (SZ) is primarily driven by discontinuous dynamic recrystallization occurring during the cooling cycle. Through the use of Electron Backscattering Diffraction (EBSD), the authors further demonstrated that the textural patterns in the SZ are defined by {111}<uvw> and {hkl}<110> partial simple shear fiber textures. Understanding such textural evolution is vital for predicting the anisotropic mechanical behavior of the joint, especially when transitioning to dissimilar interfaces.

Currently, a major frontier in FSW innovation is the joining of dissimilar materials [12]. This is particularly critical for hybrid structures that require the localized corrosion resistance of stainless steel paired with the specialized properties of other high-performance alloys. However, research involving the steel family remains disproportionately limited, with studies focused on stainless steel dissimilar connections, especially to Nickel (Ni), Titanium (Ti), and Nitinol (NiTi), being even scarcer. This gap in literature represents a significant barrier to the industrial adoption of multi-material systems. The industrial drive for fuel efficiency and environmental sustainability has pushed research toward hybrid structures, as reviewed by Patel et al. [13], who emphasized the importance of steel-aluminum systems in reducing vehicle weight.

The challenges of such systems are often rooted in the disparate flow behaviors of the materials involved. The study of Jafarzadegan et al. [14] on the dissimilar FSW of AISI 304 stainless steel to St37 steel illustrate that the mechanical interlocking and the resulting grain refinement are heavily dependent on the positioning of the harder material relative to the tool's rotation. These investigations reveal that the stir zone undergoes intense plastic deformation, where the chemical gradient between the two alloys can lead to heterogeneous microstructures that dictate the overall joint strength. If joining two different grades of steel already presents such interfacial complexity, the challenge is further magnified when stainless steel is paired with highly reactive alloys like Titanium or Nickel. In these cases, the maintenance of the stainless steel's inherent properties during the joining process is a primary concern. Li et al. [15] demonstrated that even in high-quality FSW joints of nitrogen-enriched austenitic steels, the thermal cycle can trigger the precipitation of $Cr_{23}C_6$ carbides and the formation of δ-ferrite. These microstructural alterations, as the authors observed, may lead to a localized reduction in pitting and intergranular corrosion resistance. Such findings emphasize that when joining stainless steel to highly reactive dissimilar alloys like Ti or NiTi, the control over the interfacial chemistry becomes even more critical to avoid not only mechanical embrittlement but also accelerated chemical degradation.

The disparity in thermophysical properties between stainless steel and these alloys complicates the interfacial bonding, often leading to the formation of brittle intermetallic compounds (IMCs) and asymmetric material flow. This article provides a comprehensive overview of the current state-of-the-art regarding the Friction Stir Welding of stainless steel to dissimilar high-performance alloys, specifically Nickel (Ni), Titanium (Ti), and Nitinol (NiTi). The analysis transcends traditional microstructural and mechanical characterization by evaluating the interplay between critical process parameters, such as the rotation-to-traverse ratio, and the resulting chemical gradients at the interfacial zones. Furthermore, to provide a strategic engineering perspective, a SWOT analysis (Strengths, Weaknesses, Opportunities, and Threats) is systematically conducted for each joint category. This dual approach allows for the identification of critical success factors, such as the suppression of specific intermetallic phases and the preservation of Nitinol's shape memory effects, while highlighting the technological barriers and market opportunities for these heterogeneous structures in extreme-environment applications.

2. Methodology

To ensure a robust and systematic analysis of the FSW of dissimilar stainless-steel joints, this study followed a multi-step methodological framework. The review process was designed to synthesize findings from approximately 95 core peer-reviewed articles, ensuring both breadth and technical depth.

2.1. Literature Selection and Data Acquisition

The research was conducted across major scientific databases (e.g., ScienceDirect, SpringerLink, and Scopus), focusing on peer-reviewed articles published in the last 20 years. The selection criteria prioritized:

- Material Pairings: Stainless steel (austenitic and superaustenitic) joined to Nickel (Ni), Titanium (Ti), and Nitinol (NiTi).
- Process Parameters: Studies providing quantitative data on rotational speed (RPM), traverse speed (mm/min), and tool geometry.
- Characterization Techniques: Articles employing advanced microscopy (EBSD, TEM), mechanical testing (tensile, microhardness), and electrochemical analysis (corrosion).

Inclusion Criteria: Studies were selected based on (1) material pairings: austenitic/superaustenitic stainless steel with Ni, Ti, or NiTi; (2) availability of quantitative process parameters and (3) reported mechanical/metallurgical characterization.

Exclusion Criteria: Non-peer-reviewed conference abstracts, grey literature, and studies lacking comprehensive interfacial microstructural or mechanical data were excluded to maintain the review's analytical quality.

2.2. Comparative Parameters and Interfacial Analysis

Data extraction followed a standardized protocol where findings were categorized into three analytical pillars:

(1) Interfacial Kinetics: Growth laws of IMC layers and diffusion-controlled phenomena.
(2) Microstructural Evolution: Analysis of DRX mechanisms (dDRX, cDRX, and coupled transformations).
(3) Mechanical/Functional Reliability: UTS, toughness, and transformation stability.

Extracted data were correlated using the heat input index to standardize comparisons across disparate experimental setups.

2.3. SWOT Analysis Framework

To bridge the gap between laboratory research and industrial application, a SWOT (Strengths, Weaknesses, Opportunities, and Threats) analysis was developed for each material pairing. The criteria for the SWOT matrix included:

- Technical Performance: Joint efficiency, grain refinement, and phase stability.
- Economic Feasibility: Tool wear rates and processing time.
- Innovation Potential: Compatibility with aerospace and biomedical standards.

3. State-of-the-Art in Dissimilar Friction Stir Welding of High-Performance Alloys

3.1. Fundamentals of the Friction Stir Welding (FSW) Process

Friction Stir Welding (FSW) is a thermo-mechanical solid-state joining process governed by localized frictional dissipation and intensive plastic deformation. Unlike conventional welding, the metallurgical bond is achieved through the coupling of thermal softening and a constrained material flow [16]. The process architecture involves a non-consumable, high-strength tool—comprising a specially profiled pin and a shoulder—which is plunged into the joint line while rotating at a specific angular velocity [17]. The fundamental architecture of the process, including the interaction between the rotating tool and the workpieces, is illustrated in Figure 1.

The tool serves two primary functions: (i) the shoulder-workpiece interaction generates the majority of the frictional heat, inducing a localized reduction in the material's yield strength; and (ii) the rotating pin acts as a mechanical impeller, facilitating the solid-state extrusion of the plasticized material around the tool's geometry. This transport mechanism moves material from the leading edge to the trailing edge, where it is consolidated under high hydrostatic pressure to form the weld nugget [17].

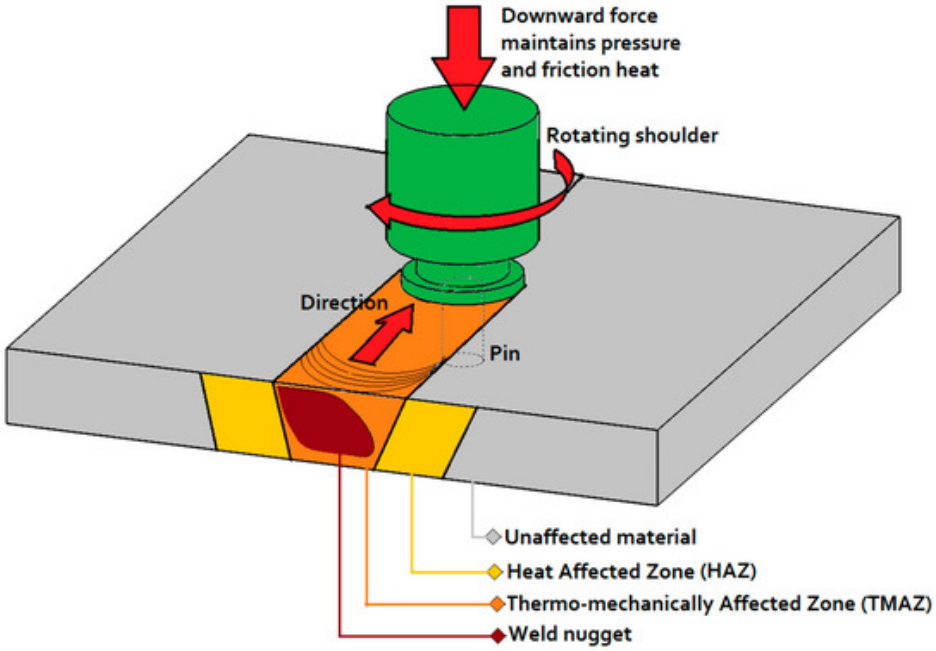

Figure 1. Schematic illustration of the Friction Stir Welding (FSW) process, highlighting the rotating tool components and the characteristic microstructural zones (HAZ, TMAZ, and Weld Nugget). Reproduced from [17].

A critical advantage of FSW is its operating temperature, which typically ranges from 0.6 to 0.9 of the base metal's melting temperature (Tm) [18]. By remaining in the solid state, the process inherently suppresses solidification-related defects such as dendritic segregation, gas porosity, and liquation cracking—phenomena that often compromise the integrity of high-strength alloys and dissimilar couples in fusion-based methods [19]. Consequently, the resulting joint is characterized by a refined, equiaxed microstructure driven by dynamic recrystallization (DRX), which provides superior mechanical properties and minimal residual stress [20].

Fraser et al. [21], reports that, for the joining of plates by the FSW process, sequences are defined in the welding, which are divided into four different phases. Each stage plays a specific role in the welding process. The welding sequence starts with the immersion phase, passing through a stabilization phase, advancing phase and ending with the tool removal phase (Figure 2).

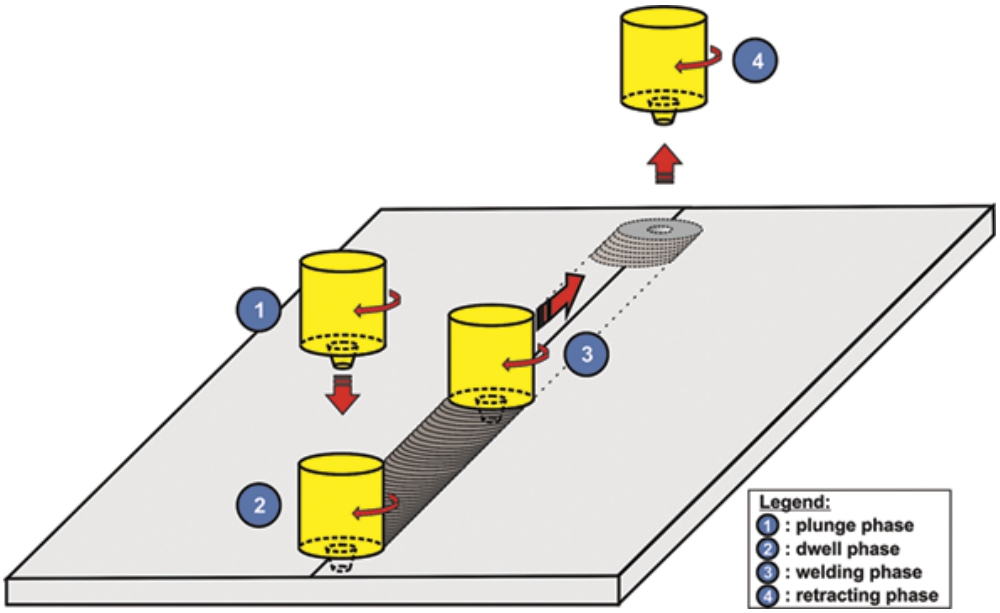

Figure 2. Welding sequence in FSW: (1) Immersion phase; (2) Stabilization phase; (3) Advancing phase and (4) Tool removing phase. Reproduced from [21].

The FSW cycle is analytically divided into four distinct stages: plunging, dwelling, traversing, and retraction [22]. Initially, the rotating tool is subjected to a controlled axial force (Fz), driving the pin into the joint interface. During

this plunging phase, the localized contact pressure and friction initiate a rapid thermal transient, increasing the temperature to a range where the material's flow stress significantly drops [23].

Once the tool shoulder achieves intimate contact with the workpiece surface, the dwelling phase begins. This stage is critical for stabilizing the thermal field and ensuring sufficient thermal softening before translation starts. It is important to emphasize that since the peak temperature remains in the solid-state regime (sub-solidus), the metallurgical union is achieved not by fusion, but through a combination of mechanical stirring and hydrostatic pressure [24].

As the tool progresses along the weld line (traversing phase), the shoulder geometry serves a dual purpose [25]:

(1) Frictional Heat Generation: Acting as the primary heat source due to its larger surface area compared to the pin.
(2) Material Confinement: Preventing the upward expulsion of the plasticized metal (flash) and ensuring that the material is forged behind the tool.

This mechanical mixing, coupled with the high strain rates induced by the tool's rotation, promotes an increase in ductility and facilitates the interfacial mass transport necessary for joining dissimilar alloys with high chemical and physical disparities [26].

Regarding the parameters controlling the quality of the welding in FSW, the following stand out: axial force, tool geometry, rotational speed, transversal speed, and angle of inclination of the tool [9]. The variation of these implies different consequences in the final welds (Table 1).

Table 1. Most influential parameters and their effects for the friction stir welding process.

Parameter	Effect
Tool rotation	Heat generated by friction; Mixing and movement of the material
Transverse speed	Weld appearance; Heat control
Advance angle	Weld appearance; Influence on thickness
Axial force	Heat generated by friction; Regulates contact conditions (tool/material)

The parameters summarized in Table 1 do not act in isolation; rather, they define the net heat input and the rheological behavior of the plasticized zone. To assess their degree of influence, we utilize a Process Sensitivity Analysis framework, where parameters are ranked by their contribution to the two governing pillars of FSW: Thermal Cycle Management and Material Flow Stability. The relationship between rotational speed (ω) and traverse speed (v) is particularly critical in dissimilar joining, as it dictates the peak temperature and the cooling rate of the weld [27]. High ω/v ratios promote excessive heat, which, while improving material fluidity, may lead to the uncontrolled growth of brittle intermetallic compounds (IMCs) at the interface [28].

- Thermal Control: The axial force and tool rotation are the primary drivers of frictional energy. While tool rotation governs the stirring intensity and shear strain, the axial force ensures the hydrostatic pressure required for solid-state consolidation [29].
- Volumetric Integrity: The advanced angle and transverse speed significantly influence the forging action of the tool shoulder [30]. A precise tilt angle facilitates the flow of plasticized metal from the front to the back of the tool, preventing common volumetric defects such as "wormholes" or "tunneling," which are prevalent when welding high-strength materials like austenitic steels [31].
- Microstructural Refinement: Collectively, these parameters control the strain rate ($\dot{\varepsilon}$) and the temperature gradient (G), which are the fundamental variables for Dynamic Recrystallization (DRX) [32]. Optimizing this parametric envelope is essential to achieve a refined grain structure in the stir zone (SZ) while maintaining the mechanical properties of the base metals.

3.2. Technological Benefits and Process Constraints

The Friction Stir Welding (FSW) paradigm offers a multifaceted array of advantages encompassing metallurgical integrity, environmental sustainability, and energy efficiency [33–35]. From a metallurgical perspective, the solid-state nature of FSW is its most significant attribute [36]. By avoiding the liquid-to-solid phase transformation, the process inherently suppresses solidification shrinkage and the associated thermal stresses, leading to a substantial reduction in macro-distortion. Furthermore, the intense plastic deformation induces dynamic recrystallization, resulting in a highly refined and equiaxed grain structure in the stir zone (SZ) with no depletion of volatile alloying elements. These characteristics enable the joining of conventionally "unweldable" dissimilar combinations—such as stainless steel to Ni, Ti, and NiTi—which are otherwise prone to catastrophic cracking in fusion-based processes. Thus, this process applies to a wide range of materials, through the variation of welding and tool parameters, even allowing dissimilar materials to be joined [34,35].

Sustainability is a hallmark of the FSW process [37]. The technology eliminates the requirement for shielding gases, filler metals, and aggressive chemical pre-treatment or post-weld cleaning, significantly reducing the carbon footprint of the manufacturing cycle [38,39]. From an energy and design standpoint, FSW enables the fabrication of "tailor-welded" structures [40]. This optimized material distribution allows for significant lightweighting in the automotive and shipbuilding sectors, directly translating to enhanced fuel efficiency and reduced greenhouse gas emissions.

Despite its disruptive potential, FSW entails specific technical constraints that must be managed [41]:

- Exit Hole (Material Gap): The withdrawal of the pin at the end of the weld path leaves a characteristic exit hole, which may require specialized "run-out" plates or "refill FSW" variants for structural applications [42].
- Fixturing and Reactive Forces: The process demands robust and high-rigidity clamping systems to withstand the significant lateral and axial forces required for pin penetration and material consolidation [43].
- Processing Hard Materials: When welding high-melting-point dissimilar alloys, such as stainless steel to Ti, the elevated flow stresses impose extreme thermal loads on the tools, necessitating expensive, high-performance tool materials (e.g., PCBN or W-based alloys) and often resulting in longer cycle times compared to aluminum FSW [44].

3.3. Dissimilar Joints and Interfacial Challenges

The FSW process exhibits remarkable versatility, having demonstrated technical feasibility across a diverse spectrum of substrates, including aluminum [44], magnesium [16], and various steel grades [45]. While its application has expanded to copper, titanium alloys [46], zinc [47], metal matrix composites [48], and even thermoplastic polymers [49], the transition from similar to dissimilar high-performance systems introduces significant metallurgical complexity.

As previously established, the primary advantage of FSW lies in its ability to produce high-integrity joints between materials with disparate chemical and thermophysical compositions, combinations often deemed "unweldable" by conventional fusion processes. In traditional fusion welding, such incompatibilities frequently trigger the formation of expansive, brittle intermetallic phases and deleterious defects, such as macroscopic porosity and solidification cracking [50].

Consequently, FSW enables the bonding of similar and dissimilar alloys with significantly different melting points without the requirement for filler materials, thereby expanding the possibilities for advanced multi-material engineering [51]. For a successful dissimilar weld to occur, particularly when pairing stainless steel with Ni or Ti alloys, the interface must satisfy two fundamental thermomechanical criteria [52,53]:

- Hot-Forging Capacity: The base materials must exhibit sufficient plastic flow at sub-solidus temperatures to allow adequate material transport and mechanical interlocking around the tool.
- Frictional Coupling: The materials must possess adequate lubricity characteristics (friction coefficient) to ensure stable heat generation during the stir phase, avoiding "slippage" that leads to cold-lap defects.

In the specific context of joining stainless steel to Nickel and Titanium, the disparity in thermal conductivity and flow stress creates an asymmetric material flow [54]. This asymmetry requires strategic tool positioning—typically offsetting the tool toward the material with lower flow stress—to balance the heat input and minimize the thickness of the Intermetallic Compound (IMC) layer. As highlighted by Patel et al. [13], managing these interfacial reactions is the key to preventing premature failure in hybrid structures designed for aerospace and biomedical applications.

3.4. Technical Impediments and Interfacial Kinetics in Dissimilar FSW

The primary complexity in joining dissimilar materials stems from the significant disparities in their thermophysical and chemical properties, specifically melting temperatures, thermal conductivities, and coefficients of thermal expansion (CTE) [55]. Unlike conventional fusion welding, where metallurgical compatibility is often managed through filler material selection, FSW operates without external additions [56]. This absence of filler material, coupled with intense plastic deformation and localized frictional heating, can trigger the formation of brittle intermetallic compounds (IMCs) at the interface [57,58]. These IMCs are the most critical challenge for structural integrity, as their thickness and morphology dictate the joint's propensity for catastrophic brittle failure [59].

From a processing perspective, the joining of heterogeneous systems can be categorized into three distinct classes based on the thermal and chemical characteristics of the substrates:

(1) Significantly Divergent Melting Points: Large thermal gradients required to plasticize the harder material (e.g., Stainless Steel) may lead to localized overheating or liquation of the softer alloy (e.g., Aluminum). As noted by Patel et al. [13], this disparity requires precise control of the heat input to avoid excessive softening.
(2) Comparable Melting Points with Distinct Chemistries: In systems like Steel-Titanium or Steel-Nickel, where melting ranges are relatively close, the challenge shifts to chemical affinity. High temperatures and intense stirring facilitate the rapid diffusion-driven growth of IMCs. Li et al. [15] observed that even small microstructural shifts, such as the precipitation of $Cr_{23}C_6$, can significantly alter the chemical stability and mechanical toughness of the interface.
(3) Near-identical Melting Ranges with Rheological Disparity: Where the challenge shifts from thermal management to mechanical flow compatibility. Even with similar melting points, differences in flow stress can result in asymmetric material transport. Mironov et al. [11] emphasized that the crystallographic texture and grain refinement in these zones are governed by discontinuous dynamic recrystallization, which must be balanced across the interface to ensure a cohesive metallurgical bond.

3.5. Material Selection and Thermophysical Characterization

3.5.1. Stainless Steel: Metallurgical Classification and Passivity

Stainless steels are iron-based alloys primarily characterized by a minimum Chromium (Cr) content of approximately 11–12%. This threshold is critical for establishing effective corrosion resistance across diverse environments, stemming from the material's ability to transition into a passive state. This passivity is facilitated by the spontaneous formation of a dense, adherent, and transparent chromium oxide (Cr_2O_3) film, typically exhibiting a thickness between 3 and 5 nm [60].

The metallurgical versatility of stainless steels allows for the enhancement of mechanical properties and chemical stability through the addition of alloying elements such as Nickel (Ni), Molybdenum (Mo), Titanium (Ti), and Manganese (Mn) [61]. However, it is noteworthy that these alloys are generally unsuitable for traditional nitriding treatments, as the process tends to deplete the matrix of free chromium, thereby compromising its inherent corrosion resistance. Historically, stainless steels are categorized into five distinct groups based on their predominant crystalline microstructure [62]:

- Ferritic: Containing 11–20% Cr and less than 0.3% C. These alloys are non-hardenable by heat treatment, offer stable atmospheric corrosion resistance, and maintain structural integrity at elevated temperatures.
- Austenitic: Characterized by 17–25% Cr and 6–20% Ni. These represent the most corrosion-resistant group; while they cannot be hardened by heat treatment, they exhibit significant work-hardening during plastic deformation.
- Martensitic: Featuring 12–18% Cr and higher carbon contents (0.1–1.2%). These steels can be quenched and tempered to achieve high hardness and resistance, making them ideal for structural components and cutting tools.
- Duplex: Composed of a balanced dual-phase structure (typically 50% ferrite and 50% austenite). Duplex steels offer a superior combination of high mechanical strength and exceptional localized corrosion resistance, finding extensive use in the petrochemical and food industries.
- Precipitation-Hardening: Alloys that achieve high strength through the formation of intermetallic precipitates within the matrix.

3.5.2. Duplex Stainless Steels (DSS): Microstructural Balance and Phase Stability

Duplex stainless steels (DSS) are characterized by a dual-phase microstructure consisting of approximately equal volume fractions of ferrite (α) and austenite (γ) [63]. This synergistic combination allows DSS to inherit stress corrosion cracking resistance of ferritic steels and the superior toughness and weldability of austenitic grades. The chemical balance of DSS is primarily driven by the interaction between iron, chromium, and nickel [64]. The microstructural stability is maintained through the strategic addition of alloying elements categorized by their phase-stabilizing behavior:

- Ferrite Stabilizers: Chromium (Cr) and Molybdenum (Mo) are the primary elements that expand the stability range of the alpha-phase [65].
- Austenite Stabilizers: Nickel (Ni), Nitrogen (N), and Copper (Cu) are employed to promote and stabilize the gamma-phase [66].

Typically, these alloys feature chromium contents ranging from 19% to 28% and nickel contents between 4% and 8%. Based on their chemical composition and Pitting Resistance Equivalent Number (PREN), duplex stainless steels are classified into four main industrial categories [67]:

(1) Lean Duplex: Low-alloy variants designed for cost-effectiveness in less aggressive environments.

(2) Standard Duplex: Medium-alloy grades (e.g., 2205) providing a versatile balance of properties.
(3) Super Duplex: High-alloy steels characterized by exceptional corrosion resistance, often comparable to super-austenitic grades with 5–6% Molybdenum content.
(4) Hyper Duplex: Highly alloyed variants developed for extreme service conditions in the petrochemical and subsea industries.

In the context of Friction Stir Welding, the solid-state nature of the process is particularly advantageous for DSS. Unlike fusion welding, where rapid solidification can lead to excessive ferritization or the precipitation of deleterious secondary phases, the controlled thermo-mechanical cycle of FSW allows for better preservation of the α/γ balance. As investigated by Saeid et al. [68], the thermal cycle of FSW allows for more controlled grain refinement in both the ferrite and austenite phases compared to fusion welding. Their research indicates that by optimizing the heat input, it is possible to maintain the 50/50 phase balance in the stir zone, effectively avoiding the excessive ferritization and the precipitation of brittle intermetallic phases, such as the sigma phase, which typically compromise the joint's toughness.

3.5.3. Titanium Alloys: Allotropic Nature and Phase Classification

Titanium alloys are categorized based on their microstructural phases, which are directly influenced by the concentration and nature of alloying elements. These elements are classified as either α-stabilizers (such as Aluminum, Oxygen, and Nitrogen) or β-stabilizers (such as Vanadium, Molybdenum, and Niobium), according to their effect on the β-transus temperature—the point of allotropic transformation from the Hexagonal Close-Packed (HCP) α-phase to the Body-Centered Cubic (BCC) β-phase [69]. Thus, titanium alloys are classified according to the phases present in their microstructure and can be classified into α, almost-α, α+β, almost-β and β [70]. Among its various applications, the aeronautical, aerospace, biomedical, naval, and chemical industries stand out [71].

- α and near-α Alloys: Characterized by superior corrosion resistance and weldability. These alloys are generally non-heat treatable and maintain structural integrity at cryogenic and moderately elevated temperatures.
- A + β Alloys (e.g., Ti-6Al-4V): The most widely used class, offering a tailored balance between mechanical strength and ductility through heat treatment. In Friction Stir Welding, these alloys undergo complex phase partitioning in the stir zone due to the thermo-mechanical cycle.
- β and near-β Alloys: These are metastable alloys that provide high formability and ductility. Their high mechanical strength is typically achieved through solid solution hardening or the controlled precipitation of fine α particles during aging [72].

In the context of dissimilar FSW with stainless steel, titanium presents a significant challenge: its high chemical affinity for Iron (Fe) and Carbon (C). When the peak temperature exceeds critical limits, diffusion-driven reactions at the interface can lead to the formation of brittle Fe-Ti intermetallics (such as FeTi and Fe_2Ti). These phases act as stress concentrators and crack initiation sites, drastically reducing the joint's ductility and causing premature failure under tensile or fatigue loading.

3.5.4. Nickel Alloys: Thermal Stability and Chemical Compatibility

Nickel is a versatile transition metal characterized by its exceptional oxidation resistance, high thermal and electrical conductivity, and excellent ductility [73]. In industrial applications, nickel is frequently employed in marine engineering and food processing equipment due to its ability to maintain a stable passive surface in aggressive environments [74].

Nickel alloys are engineered to withstand extreme thermomechanical conditions, maintaining their mechanical strength and creep resistance at elevated temperatures. These alloys are systematically categorized into four main groups [75]:

- Binary Alloys (e.g., Ni-Cu): Known for their high corrosion resistance in seawater.
- Ternary and Complex Alloys: Developed for specialized chemical environments.
- Nickel-based Superalloys: Advanced systems designed for the aerospace and turbine industries, where structural integrity at temperatures exceeding 0.7Tm is mandatory.

In the context of Friction Stir Welding, Nickel and its alloys present a unique metallurgical advantage when paired with austenitic stainless steels. Since Nickel acts as a potent austenite-stabilizing element (γ-genics), the chemical gradient across a Steel-Ni interface exhibits inherent thermodynamic compatibility, significantly reducing the risk of phase instability compared to the more reactive Steel-Ti systems.

As highlighted by Lemos et al. [76], the industrial demand for FSW in Nickel-based systems has intensified, particularly driven by the rigorous requirements of subsea engineering and deep-water hydrocarbon exploitation.

The process serves as a strategic alternative for joining Corrosion-Resistant Alloys (CRA), as its solid-state nature preserves, or in some cases enhances, the localized corrosion resistance and mechanical integrity, properties that are frequently compromised by the thermal cycles of conventional fusion welding. Their comprehensive review emphasizes that for high-performance superalloys, such as the Inconel series (600, 625, and 718), joint efficiency is intrinsically linked to the synergy between tool material technology and the resulting microstructural evolution. However, Lemos et al. [76] also denote that while FSW joints demonstrate promising performance in preliminary corrosion assays, the field faces a critical bottleneck: the development of advanced tool materials (e.g., PCBN or refractory alloys) capable of sustaining the extreme thermomechanical loads and wear rates imposed by these high-strength nickel matrices.

3.6. Friction Stir Welding of Stainless Steel to Dissimilar Alloys

Despite the strategic importance of hybrid structures, research dedicated to the Friction Stir Welding (FSW) of stainless steel to dissimilar alloys remains disproportionately scarce. This literature gap is primarily attributed to the severe thermomechanical demands of the process: the high flow stress and low thermal conductivity of stainless steels necessitate specialized tool materials (e.g., PCBN, W-based alloys) and stringent thermal management to prevent premature tool degradation. Nevertheless, pairings involving titanium and nickel have gained significant notoriety. These combinations are highly sought after in the aerospace, chemical, and nuclear sectors, as they enable the synergistic integration of the pitting corrosion resistance of stainless steel with the exceptional specific strength of titanium or the creep resistance of nickel-based superalloys.

Furthermore, recent investigations into unconventional pairings, such as stainless steel to zirconium or tantalum, have yielded promising results. These studies demonstrate the feasibility of producing defect-free joints with high structural integrity, provided that the interfacial kinetics—specifically the nucleation and growth of brittle intermetallic phases—are strictly controlled through optimized tool offset and heat input. The success of these heterogeneous joints suggests that FSW is not merely a laboratory curiosity, but a viable industrial alternative to traditional fusion welding. It allows for the fabrication of complex, multi-material components engineered to operate in aggressive environments where conventional welds would fail due to solidification cracking or chemical segregation.

3.6.1. Stainless Steel—Nickel

Recent investigations [77,78] into the heterogeneous joining of duplex stainless steels and nickel alloys have reported significant technical success, though they also highlight critical threshold defects. SS-Ni joints exhibit high ductility, characterized by fracture elongation values ranging from 20% to 30%, which significantly exceeds the requirements for structural integrity in most aerospace applications. Specifically, the occurrence of a central tunnel (wormhole) or tearing in the stir zone (SZ) has been documented when traverse speeds are excessively high, preventing the net heat input required for adequate material plasticization. Other limiting factors identified include insufficient forging pressure and a disproportionately wide thermomechanically affected zone (TMAZ) [79].

Addressing these challenges, experimental research of Thomas et al. [80]. focusing on the union between Super Duplex Stainless Steel (SDSS) 2507 and Incoloy 825 demonstrated that joint integrity is highly dependent on material positioning. The study utilized a square butt joint configuration, prepared through rigorous mechanical and chemical surface decontamination to eliminate oxides that could act as crack initiation sites. In relation to the parameters, these were varied throughout the tests, with the displacement speed and the tool rotation speed being the most frequently altered parameters. After the tests, a microscopic analysis was performed, where the authors concluded that the heat-affected zone is not distinct from the base materials. This conclusion is also confirmed by other authors. The previously mentioned tests were carried out with a displacement speed of 40 mm/min, a rotation speed of 700 rpm and with 2507 stainless steel placed on the forward side of the tool. A penetration depth of 2.8 mm and 138.28 J/mm were applied. For this sample, microhardness tests were carried out on the final piece after welding, testing non-welded areas of the two materials and welded areas of both materials (SZ: Stir Zone). Based on the tests carried out throughout their study, and considering the parameters previously defined as ideal, the authors concluded that the appearance of a weld joint without defects is possible by placing the stainless steel on the advancing side of the tool. This joint does not allow the observation of a thermally affected zone in any of the base materials, and it presents a mostly ductile fracture. Through the mechanical tests carried out, it was possible to conclude that the maximum stress and the elastic limit stress of the material are comparable to the nickel used as a base material.

Beyond the study of high-alloy systems, the interaction between different stainless-steel grades also provides critical insights into the rheological behavior of the stir zone. Mondal et al. [81] investigated the dissimilar FSW

between low-nickel austenitic stainless steel and 409M ferritic stainless steel, revealing that the material flow pattern is highly sensitive to the combination of process parameters.

Their research utilizes elemental mapping to demonstrate that the mixing of the two alloys in the stir zone is not uniform but follows a parameter-dependent morphology. A key finding of their study is the disparity in the recrystallization mechanisms:

- Ferritic Stainless Steel: Exhibits more intense dynamic recrystallization and recovery, resulting in an exceptionally fine-grained microstructure. Mondal et al. attribute this to the higher Stacking Fault Energy (SFE) of the ferritic BCC structure, which facilitates dislocation movement and grain refinement.
- Austenitic Stainless Steel: Due to its lower SFE, the austenitic phase follows a different recrystallization path, emphasizing the importance of balancing the thermomechanical input to accommodate the distinct flow stresses of each alloy.

This study reinforces the conclusion that successful dissimilar welding requires not only thermal management but also a deep understanding of the crystallographic response of each substrate to the intense plastic deformation of FSW.

A critical challenge in welding high-nickel steels (such as 9% Ni steel) via conventional fusion processes is the degradation of toughness due to chemical microsegregation and the precipitation of brittle phases. As demonstrated by Casanova et al. [82], Friction Stir Welding (FSW) offers a superior alternative by maintaining lower peak temperatures, which fundamentally alters the retention and distribution of austenite. The tool and weld joint are depicted in Figure 3.

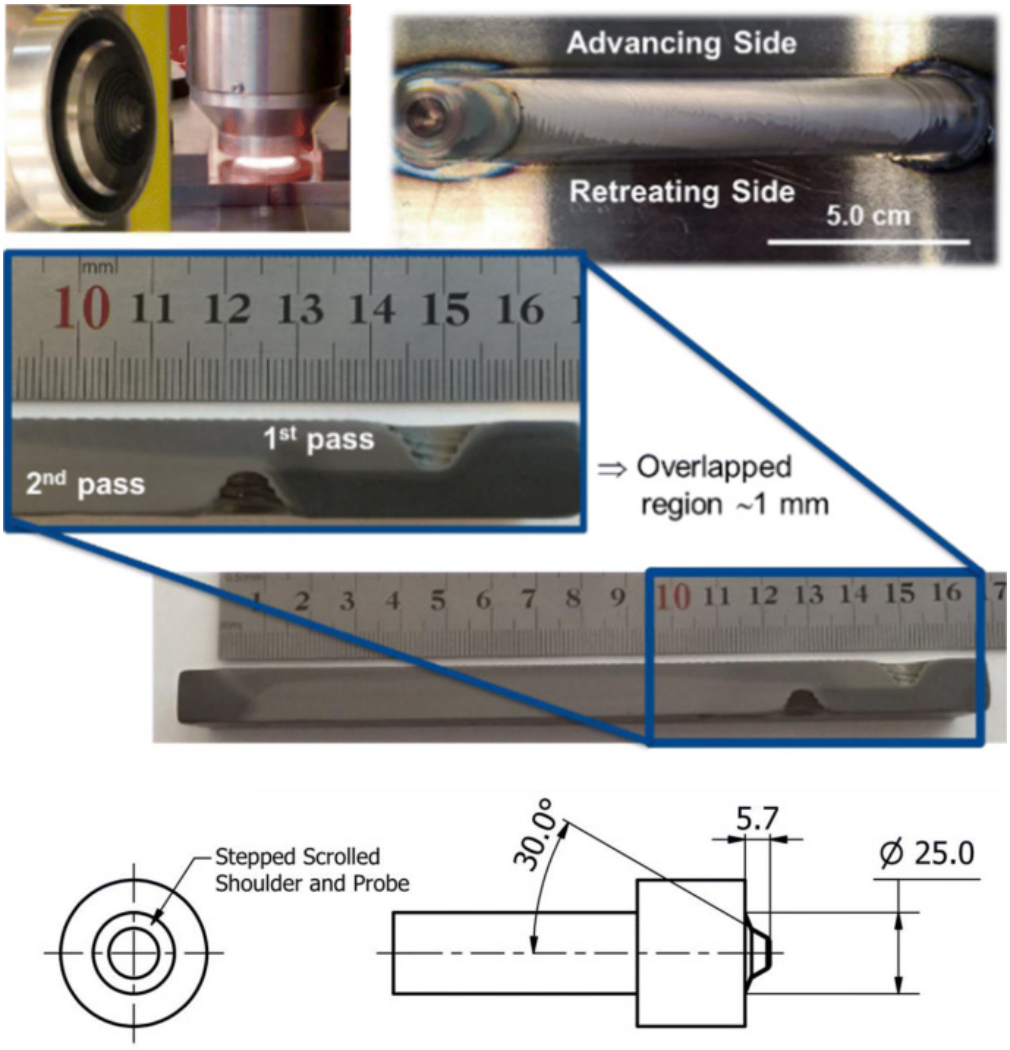

Figure 3. Technical specifications and operational overview of the FSW process: (**Top-left**) Stepped scrolled shoulder tool and the welding process in progress; (**Top-right**) Morphology of the weld bead upper surface showing the Advancing and Retreating sides; (**Center**) Longitudinal macrograph illustrating the overlap region between the first and second passes; (**Bottom**) Engineering drawing of the tool geometry with a 30.0° cone angle and 5.7 mm probe length. Reproduced from [82].

In their investigation, the role of multiple welding passes and the resulting Volumetric Fraction of Retained Austenite (VFRA) were found to be the primary drivers of mechanical performance. Key insights from their study include:

- Austenite Stability: Although the FSW process can reduce the total VFRA in the Stir Zone (SZ), the Austenite remains strategically located within deformation bands in the TMAZ, contributing to the overall structural integrity.
- Toughness Optimization: The application of a second welding pass was shown to increase the energy absorbed in Charpy V-notch tests by 17% in the initial stir zone. This thermal refinement results in an energy absorption capacity only 23% lower than the base metal, a significant improvement over laser or electron beam autogenous welding.
- Predictive Factors: The research establishes a direct correlation between the grain size, the VFRA, and the Martensite-Austenite (MA) constituent volume fraction as the significant factors for predicting the impact toughness of the joint.

This highlights that for Ni-rich systems, FSW not only provides a solid-state bond but also allows for the "tuning" of the microstructure (via multiple passes or parameter control) to meet the rigorous toughness requirements of the cryogenic and oil industries.

The transition toward nickel-free austenitic stainless steels, which utilize Nitrogen as a primary austenite stabilizer, introduces new variables to the FSW thermal cycle. Li et al. [15] demonstrated the feasibility of welding these high-performance alloys using Tungsten-Rhenium (W-Re) tools, achieving high-quality joints at optimized parameters (ω = 400 rpm; v = 100 mm/min).

Despite the solid-state nature of the process, the study highlights localized microstructural shifts that can influence the chemical longevity of the joint:

- Precipitation of Carbides: TEM analysis revealed the presence of $Cr_{23}C_6$ precipitates (approx. 1 μm) within the Stir Zone. Although the volume fraction was small, these carbides can induce localized chromium depletion.
- Phase Transformation: An increase in δ-ferrite content was observed in the SZ, which, coupled with the carbide precipitation, resulted in a slight reduction in both pitting and intergranular corrosion resistance compared to the base metal.
- Mechanical Reinforcement: Conversely, the intense grain refinement via dynamic recrystallization led to a significant increase in hardness and tensile strength in the SZ, ensuring that tensile failure occurred in the base metal (BM), thereby validating the joint efficiency from a structural standpoint.

This research underscores that for stainless steels, the "success" of FSW must be measured through a dual lens: the mechanical gain from grain refinement versus the electrochemical risk posed by minor phase transformations and precipitates.

In summary, the friction stir welding of stainless steel to nickel alloys represents a highly viable metallurgical pairing, provided there is rigorous control over the thermomechanical cycle. The body of research—ranging from the analysis of 9% Ni steels to nitrogen-stabilized austenitic grades—demonstrates that the process successfully overcomes the limitations of fusion welding by minimizing chemical microsegregation and preventing the massive precipitation of brittle intermetallics. While challenges remain regarding tool wear and the localized precipitation of $Cr_{23}C_6$ carbides, the significant grain refinement in the stir zone and the preservation of retained austenite ensure a joint with superior impact toughness and mechanical strength. Ultimately, the successful integration of these materials depends on a strategic balance between rotation and traverse speeds to optimize heat input, positioning FSW as a key technology for the next generation of high-performance components in the cryogenic and subsea industries.

SWOT Analysis: Dissimilar FSW of Stainless Steel to Nickel Alloys

The strategic evaluation of joining Stainless Steel (SS) to Nickel Alloys via Friction Stir Welding (FSW) reveals a high potential for industrial integration due to the favorable metallurgical synergy between the two FCC (Face-Centered Cubic) materials. To evaluate the strategic viability of this joining process, a comprehensive assessment was performed. Figure 4 illustrates the SWOT matrix for the dissimilar FSW of stainless steel and nickel alloys, highlighting the interplay between metallurgical strengths and operational challenges.

The SWOT analysis underscores that the feasibility of dissimilar Friction Stir Welding (FSW) between stainless steel and nickel alloys is fundamentally rooted in their high metallurgical compatibility. As both materials share a Face-Centered Cubic (FCC) crystal structure, the interface benefits from a stable chemical gradient. This inherent synergy acts as a primary Strength, allowing for a joint that maintains phase stability and avoids the catastrophic embrittlement often observed in fusion-welded dissimilar systems where brittle intermetallic compounds are prevalent.

Figure 4. SWOT analysis of the dissimilar Friction Stir Welding (FSW) between stainless steel and nickel alloys.

However, the transition from laboratory success to industrial adoption faces significant Weaknesses, primarily centered on the thermomechanical demands of the process. The high flow stress of these alloys at elevated temperatures leads to rapid tool degradation, a factor that directly impacts the cost-effectiveness of the operation. Furthermore, while FSW is a solid-state process, the risk of localized microstructural shifts, such as chromium carbide precipitation, remains a critical concern. Even minor precipitation at the grain boundaries can compromise the pitting corrosion resistance, a vital property for the Opportunities identified in the Subsea and Oil & Gas sectors.

From a mechanical perspective, the Opportunities are bolstered by the exceptional toughness achievable through solid-state joining. The ability of FSW to refine grain structures through dynamic recrystallization and to preserve retained austenite provides a pathway for high-performance applications in Cryogenic Engineering, where fracture toughness is a critical requirement. The energy absorption in the stir zone remains highly competitive with the base metals, positioning this technique as a superior alternative for environments where structural integrity under extreme conditions is non-negotiable.

Ultimately, the primary Threat to the widespread implementation of this pairing is the current lack of international standardization and the high cost of advanced tool materials capable of sustaining the process. To mitigate these risks, the strategic focus must remain on optimizing the “process window”, balancing rotation and traverse speeds to maximize joint efficiency while extending tool life. This strategic balance will be the deciding factor in moving this technology from specialized high-end applications to broader industrial manufacturing.

3.6.2. Stainless Steel—Titanium

Recent investigations into the Friction Stir Welding (FSW) of stainless steel to titanium alloys have demonstrated promising outcomes, particularly in lap joint configurations. A critical variable identified in the literature [83,84] is the vertical stacking sequence of the base materials, specifically, the positioning of the titanium or stainless-steel plate relative to the tool shoulder.

In studies utilizing AISI 304 stainless steel and Commercially Pure Titanium (Cp-Ti), the sequence proved decisive for mechanical integrity:

- Ti as Upper Plate: When the titanium plate occupied the upper position (contacting the tool shoulder), macroscopic defect-free zones were achieved. However, mechanical testing revealed a 27% reduction in shear strength relative to the base titanium’s nominal strength.
- SS as Upper Plate: Conversely, placing the titanium as the lower plate not only yielded defect-free joints but also achieved a shear strength of approximately 119 MPa. This value is substantially closer to the parent material’s performance, suggesting that placing the harder material (stainless steel) in direct contact with the tool shoulder optimizes the frictional heat generation and subsequent material flow at the interface.

Microstructural analysis confirms that FSW induces extreme grain refinement through dynamic recrystallization. In the stir zone, grain sizes were observed to reduce from 75 μm in the base material to

approximately 2 μm at the interface. Despite this refinement, the formation of intermetallic compounds (IMCs) remains the primary metallurgical challenge. The thickness of the Titanium-Iron (Ti-Fe) intermetallic layer is highly sensitive to the process parameters; research indicates that the IMC layer thickness increases proportionally with higher rotation and traverse speeds, which elevate the peak temperature and accelerate interfacial diffusion. The growth kinetics of the Fe-Ti interface reaction layers are governed by the diffusion of atomic species across the interface, which can be expressed by the parabolic growth law $X^2 = kt$, where k is the temperature-dependent rate constant. In FSW, the high strain rate and dynamic recrystallization introduce a high dislocation density, which significantly enhances the effective diffusion coefficient (D_{eff}) through lattice defects, a process known as pipe diffusion.

Optimization of the processing window is vital for balancing bond strength against IMC growth. Data indicates that for 4 mm thick specimens, the most favorable results were obtained at:

- Rotation Speed (ω): 1100 rpm
- Traverse Speed (*v*): 50 mm/min

These parameters provided the necessary thermal input for plasticization while keeping the interfacial kinetics within limits that prevent excessive embrittlement.

Complementing the study of stacking sequences, Fazel-Najafabadi et al. [85] investigated the internal morphology of defect-free lap joints between CP-Ti and 304 Stainless Steel. By positioning the titanium as the upper plate (the softer material), the authors identified a distinct dual region stir zone (SZ):

(1) Upper Region: Dominated by a refined microstructure of dynamically recrystallized titanium grains.
(2) Lower Region: Characterized by a composite-type microstructure, where fragments of 304 stainless steel are embedded within a matrix of ultra-fine titanium grains.

The most critical finding of this research is the presence of a TiFe-based crystal structure at the interface separating the stir zone from the stainless-steel base metal. This intermetallic layer serves as the primary site for crack initiation and propagation.

Key results from this study include:

- Joint Efficiency: The maximum failure load achieved was approximately 73% of the CP-Ti base metal strength.
- Fracture Mechanism: Failure predominantly occurred at the intermetallic-based interface, rather than within the stir zone or the base materials.
- Layer Thickness Correlation: There is a direct inverse relationship between the thickness of the TiFe intermetallic layer and the joint's shear strength; as the heat input increases the layer's thickness, the failure load significantly decreases.

A more granular understanding of interfacial chemistry was provided by Ishida et al. [86], who mapped the reaction layers formed during the dissimilar FSW of CP-Ti and 304 Stainless Steel (SUS304). Their study highlights that the thickness and complexity of the interface are highly sensitive to the joining speed, which dictates the diffusion time and thermal cycle.

At an optimized joining speed of 50 mm/min, a flat and stable interfacial reaction layer was achieved with a thickness of less than 1 μm. Despite its thinness, this layer is composed of four distinct sub-layers, ordered from the titanium side to the stainless-steel side:

(1) β-Ti (+ ω-Ti)
(2) Ti_2N
(3) FeTi + Fe_2Ti
(4) σ-FeCr (Sigma phase)

The presence of the σ-FeCr and Fe_2Ti phases is particularly noteworthy, as these are notoriously brittle constituents that can act as initiation points for cleavage fracture.

The research demonstrated a significant disparity in joint performance depending on the loading condition:

- Tensile Shear Test: At all tested joining speeds, the joints were robust enough to cause fracture in the CP-Ti base material, indicating high shear integrity.
- Peel Test: Conversely, during peeling, fractures occurred directly at the joint interface. This reveals that while the interface can sustain longitudinal shear, its resistance to normal (out-of-plane) stresses is limited by the brittle nature of the thin reaction layers.

While lap joints are common, Gotawala et al. [87] explored the microstructural evolution in friction stir butt welding of SS 304 and CP-Ti. This research provides a detailed mapping of the interface using EBSD and EDS, revealing how the temperature distribution across the thickness of the plate dictates the mechanical performance of the union.

The intense heat generated during the process facilitates a bidirectional diffusion: iron, chromium, and nickel migrate into the titanium matrix, while titanium diffuses into the stainless steel. This chemical exchange results in an interface characterized by:

- β-titanium matrix with dispersed λ-Ti precipitates.
- The formation of the FeTi intermetallic compound on both sides of the interface.

A significant finding of this study is the non-uniformity of the intermetallic layer. The thickness of both the FeTi layer and the β-titanium zone decreases from the top surface to the bottom of the joint. This is directly attributed to the higher peak temperatures near the tool shoulder (top) compared to the weld root (bottom).

The research confirms the critical role of rotation speed (ω) in controlling the interfacial kinetics:

- Lower Rotation Speeds: Result in lower peak temperatures and a thinner FeTi layer, achieving an Ultimate Tensile Strength (UTS) of approximately 88% of the CP-Ti base metal.
- Brittleness Constraint: Despite the high tensile strength, the fracture strain (ductility) remained very low in all specimens. This inherent brittleness is a direct consequence of the FeTi intermetallics, which act as a continuous path for brittle fracture regardless of the optimized strength.

To extend the understanding of functional performance, Sujith K et al. investigated the mechanical and tribological properties of FSW joints using SS 310 and the advanced titanium alloy Ti-6Al-3Nb-2Zr-1Mo (Ti6321). This study is particularly relevant for aerospace and orthopedic applications, where weight reduction and surface integrity are critical.

The research compared similar (Ti-Ti) and dissimilar (Ti-SS) joints, identifying that process parameters and tool geometry (specifically pin diameter) are the primary drivers of joint quality. Under optimized conditions (ω = 900 rpm, v = 60 mm/min, and an axial force of 1 kN), the study observed:

- Microhardness: A peak of 362 HV in the stir zone, significantly higher than the base materials due to the uniform distribution of refined particles and precipitates.
- Tensile Strength: High-strength results reaching 927 MPa for similar titanium joints, providing a benchmark for the potential of FSW in high-performance alloys.

A unique contribution regarding this work is the evaluation of wear resistance using a pin-on-disc apparatus. The findings indicate:

- Wear Mechanisms: The tribological characteristics are heavily influenced by the tool diameter and welding parameters. Surface morphology via FE-SEM revealed that the Heat-Affected Zone (HAZ) is composed of acicular α phases, which influence the friction coefficient and material loss during sliding.
- Phase Analysis: XRD analysis confirmed that the increase in hardness within the Stir Zone (SZ) is attributed to the intense grain refinement and the specific phase transformations occurring under the high-strain conditions of FSW.

Moreover, the joining of Ti6Al4V titanium alloy to 30CrMnSiNi2A medium carbon steel represents a significant challenge due to the drastic differences in thermo-physical properties. Li et al. [88] successfully demonstrated that linear friction stir butt-welding can produce defect-free joints by precisely controlling the travel speed (v) at a constant rotation (ω) of 750 RPM.

A key finding of this research is the inverse relationship between travel speed and the growth of the interfacial reaction layer:

- Optimal Interface: At a higher travel speed of 75 mm/min, an optimal reaction layer of approximately 1 μm was formed, which is considered the "gold standard" for avoiding interfacial embrittlement.
- Excessive Growth: Conversely, at lower speeds (47.5 mm/min), the reaction layer reached thicknesses between 5 and 60 μm.

The authors highlight a critical phenomenon: butt welds consistently exhibit thicker reaction layers than lap welds under similar parameters. This is attributed to the higher localized peak temperatures achieved in the butt configuration, where heat dissipation is more constrained than in the overlapping plate geometry.

Using Micro-XRD, the study confirmed the presence of the FeTi intermetallic compound at the interface, which dictates the fracture path. Despite the presence of these brittle phases, the joints produced within the 47.5–75 mm/min range showed:

(1) High Tensile Strength: Values exceeding the strength of the steel base material.
(2) Fracture Localization: Failure occurred either in the TMAZ/HAZ on the steel side or at the Ti-side interface, depending on the thickness of the reaction layer.

Thus, the friction stir welding of stainless steel to titanium alloys is a complex thermomechanical process where joint efficiency is dictated by the precise control of the interfacial reaction layer. While the solid-state nature of FSW is effective in mitigating the typical defects of fusion welding, the inevitable formation of Fe-Ti intermetallics and brittle phases like σ-FeCr remains the primary challenge, driven by thermally activated diffusion mechanisms at the interface. The literature demonstrates that by optimizing the stacking sequence and maintaining a high traverse-to-rotation speed ratio, it is possible to restrict the reaction layer to a sub-micron scale (approximately 1 μm). This threshold, particularly effective for thin-gauge sheets under monotonic loading, minimizes the brittle-to-ductile transition in the joint interface, ensuring high tensile strength and superior shear integrity. However, the inherent brittleness of the interface, particularly under peel or normal stress, suggests that these joints are best suited for applications where longitudinal loading predominates. Ultimately, mastering the interfacial kinetics through precise thermal field distribution is the key to unlocking the full potential of these hybrid structures in the aerospace and power generation sectors, aligning with the latest requirements for damage-tolerant multi-material systems.

SWOT Analysis: Dissimilar FSW of Stainless Steel to Titanium Alloys

The strategic integration of Stainless Steel (SS) and Titanium (Ti) through Friction Stir Welding is characterized by a high degree of technical complexity due to the formation of brittle intermetallic compounds (IMCs). The transition from stainless steel–nickel to stainless steel–titanium systems introduces a significant increase in metallurgical complexity, primarily due to the high reactivity between Iron and Titanium. To evaluate the technical and industrial viability of this specific coupling, a comprehensive strategic assessment was conducted. Figure 5 presents the SWOT analysis for the dissimilar Friction Stir Welding of stainless steel and titanium alloys, synthesizing the trade-offs between mechanical strength and interfacial brittleness.

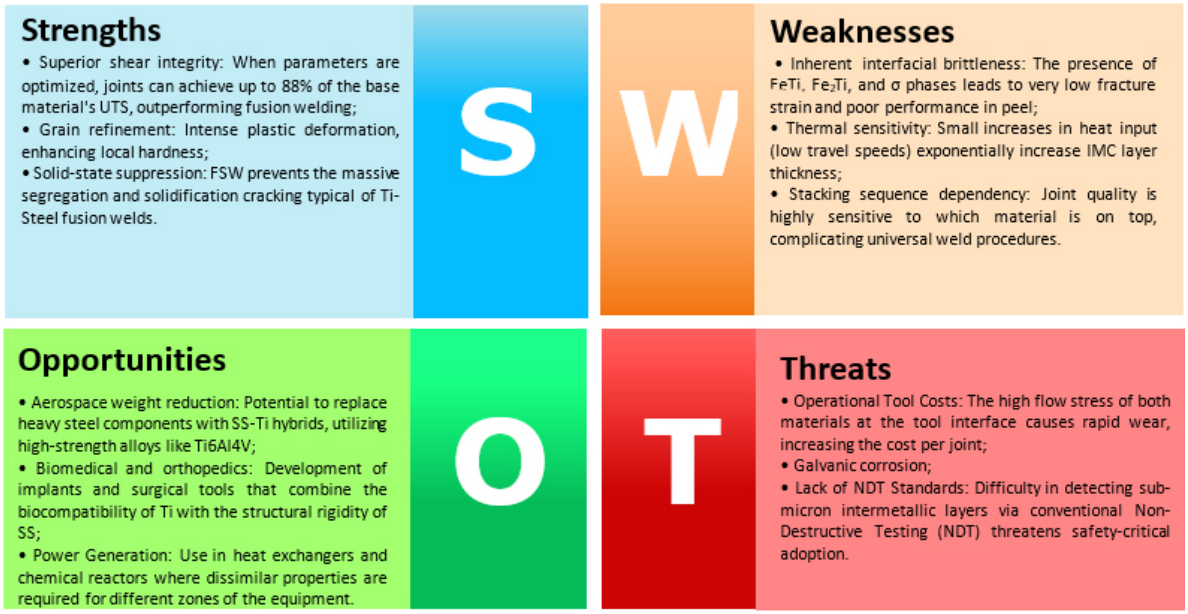

Figure 5. SWOT matrix for the dissimilar Friction Stir Welding (FSW) of Stainless Steel and Titanium alloys.

The strategic landscape for the Friction Stir Welding of stainless steel to titanium reveals a paradigm shift compared to more compatible systems like steel-nickel. The core of this discussion lies in the dynamic between metallurgical strength and interfacial brittleness. While the process is categorized as a solid-state technique, the high temperatures reached near the tool shoulder trigger a chemical diffusion that is both the source of the bond and the primary cause of its potential failure.

The Strengths identified—specifically the ability to reach up to 88% of the base material's Ultimate Tensile Strength (UTS) are a testament to the effectiveness of dynamic recrystallization and the creation of a "composite-type" microstructure in the stir zone. However, this mechanical performance is highly conditional. As seen in the Weaknesses section, the joint's integrity is extremely sensitive to the "thermal dose." A critical threshold exists once the FeTi and Fe_2Ti intermetallic layer exceeds a thickness of 1 μm, the joint transitions from a high-strength bond to a fragile interface prone to cleavage.

Furthermore, the discussion must address the rheological mismatch mentioned in the analysis. The difference in flow stress between the harder stainless steel and the relatively softer titanium requires a strategic "stacking sequence." Placing the harder material in contact with the tool shoulder optimizes heat generation, but it also increases the risk of tool wear—a significant Threat to the commercial scalability of this process.

From an industrial perspective, the Opportunities in weight-sensitive sectors like aerospace and orthopedics are vast. However, the Threat of galvanic corrosion and the lack of specialized non-destructive testing (NDT) for sub-micron layers cannot be ignored. The success of this dissimilar coupling depends on a design philosophy where the joint is subjected primarily to shear loads. In applications where peeling or normal stresses are present, the brittle nature of the Ti-Fe and σ phases (identified by XRD and EBSD) could lead to premature failure even if the nominal tensile strength is high.

In summary, the SWOT analysis indicates that the SS-Ti FSW joint is a "high-performance/high-maintenance" solution. It offers superior properties to fusion welding but requires a much narrower processing window and more sophisticated monitoring to ensure that the interfacial chemistry remains within the limits of structural safety.

3.6.3. Stainless Steel—Nickel Titanium (NiTi)

Nickel-Titanium (NiTi) alloys, commonly categorized as Shape Memory Alloys (SMAs), are distinguished by their unique capability to recover a pre-defined geometry through thermal activation or superelastic damping [89]. Despite these superior functional properties, their widespread industrial adoption has been historically hindered by the metallurgical challenges of joining them to dissimilar metals, specifically the risk of compromising their martensitic transformation temperatures through excessive heat input.

Recent research, of Zhi-Hong et al. [90] has explored the viability of bonding NiTi to AISI 304 stainless steel using FSW, employing a low-heat-input regime (ω = 400 rpm; v = 75 mm/min). The microstructural characterization revealed significant dynamic recrystallization, producing a refined grain structure within the stir zone. A critical finding was the thermal asymmetry of the joint:

- NiTi Side: The Thermo-Mechanically Affected Zone (TMAZ) was exceptionally narrow, and the Heat-Affected Zone (HAZ) was nearly indistinguishable. This localization is vital, as it prevents the "erasing" of the shape memory effect and maintains the stability of the transformation temperatures.
- Stainless Steel Side: The microstructure followed the typical evolution of austenitic steels under FSW, showing a characteristic softened zone.

Vickers microhardness testing across the interface demonstrated distinct behaviors: the stainless-steel side experienced localized softening compared to its base metal, while the NiTi side maintained constant hardness values throughout the transition. Despite the successful mixing of the two materials, demonstrating high metallurgical compatibility, the study noted the occurrence of tunnel defects along the weld line. These defects are often attributed to the significant disparity in the flow stress (rheological mismatch) between the austenitic stainless steel and the NiTi alloy during the solid-state stirring. However, the overall results confirm that FSW is a highly promising technique for creating functional hybrid components without the catastrophic loss of superelasticity.

To quantify the retention of the shape memory effect, Prabu et al. [91] conducted a comprehensive study on the FSW of austenitic NiTi alloys. Their research bridges the gap between microstructural refinement and functional performance, utilizing Differential Scanning Calorimetry (DSC) to monitor phase transformation behaviors and Finite Element Analysis (FEA) to map temperature distribution.

The study demonstrated that NiTi joints welded at rotational speeds of 800 and 1000 rpm successfully retained their superelastic plateau during tensile testing. This indicates that the stress-induced martensitic transformation, which is the core of NiTi's functionality, remains active despite the thermomechanical processing of FSW.

Key functional findings include:

- Transformation Temperature Drift: Only a marginal shift in transformation temperatures was observed, ensuring that the alloy's operational range remains largely unchanged.
- Shape Recovery: The welded joints exhibited complete time-dependent shape recovery, returning to their original geometry after 27 s at a temperature of 65 °C.

Through FEA, the researchers correlated the stability of the Nitinol phases with the controlled heat input of the process. The grain refinement caused by dynamic recrystallization in the stir zone did not impede the atomic movements required for shape memory. This confirms that the solid-state nature of FSW is uniquely suited for NiTi, as it avoids the massive heat-affected zones and elemental segregation that typically destroy SMA properties in fusion welding.

To consolidate the current understanding of Nitinol welding, the comprehensive review by Datta and Biswas [92] emphasizes that the preservation of the pseudoelastic effect and shape memory properties is directly linked to the chemical stability of the joint. In fusion-based processes, NiTi alloys are highly susceptible to compositional variations due to the volatilization of alloying elements, which fundamentally alter their functional response.

The primary advantage of Friction Stir Welding, as highlighted by the authors, is its operation below the melting point of the base materials. This solid-state nature ensures:

- Compositional Integrity: Avoidance of nickel or titanium loss, ensuring that the Ni/Ti ratio—which governs the transformation temperatures, remains constant.
- Structural Flexibility: The ability to create complex geometries in both similar and dissimilar combinations, providing the design flexibility required for advanced manufacturing.

Beyond mechanical strength, the review underscores the importance of corrosion resistance and smart functionality in welded structures. The localized thermomechanical cycle of FSW minimizes microstructural degradation, which:

(1) Enhances Fatigue Life: Crucial for biomedical implants and actuators subject to cyclic loading.
(2) Maintains Corrosion Barriers: Prevents the formation of secondary phases that could act as initiation sites for localized corrosion in saline or acidic environments.

Ultimately, the work of Datta and Biswas [92] positions FSW as the most viable method for integrating NiTinol into "smart" hybrid structures, satisfying the stringent requirements of metallurgy, mechanics, and functional longevity.

Beyond standard FSW, the work of Shashikala et al. [93] explores the application of Rotary Friction Welding (RFW) on superelastic NiTinol rods, providing a benchmark for the mechanical limits of friction-based joining. A significant contribution of this research is the quantification of how post-welding treatments, specifically heat treatment and cryogenic treatment, can further enhance the joint's performance.

The study revealed that the "as-welded" state is merely a baseline, and substantial improvements can be achieved through controlled thermal cycles:

- Tensile and Flexural Strength: After heat treatment, the joints achieved a maximum tensile strength of 1112 MPa, representing an increase of up to 37% compared to the non-treated samples at optimized speeds (1900 rpm). The flexural strength followed a similar trend, peaking at 3.29 kN/mm².
- Impact Resistance: Heat-treated samples showed a remarkable increase in impact strength (up to 57% higher), which is crucial for components subject to dynamic loading.

The research also introduced cryogenic treatment as a method to refine the hardness profile. The highest microhardness of 347 HV was recorded for cryogenically treated samples, outperforming both heat-treated and as-welded counterparts.

These findings suggest that for high-performance applications, the friction welding process should be viewed as part of a broader manufacturing sequence where post-processing plays a decisive role in achieving the full mechanical potential of the NiTinol alloy.

SWOT Analysis: Dissimilar FSW/RFW of Stainless Steel to Nitinol

The integration of Shape Memory Alloys (SMAs) with structural steels represents the state-of-the-art in materials engineering, where the objective shifts from simple mechanical bonding to the creation of "smart" or functional hybrid components. The strategic landscape for the Friction Stir Welding of stainless steel to Nitinol is summarized in Figure 6. This SWOT analysis highlights the trade-off between maintaining the alloy's functional properties and overcoming the mechanical challenges of the process.

The strategic landscape highlights a fundamental shift in priorities when transitioning from conventional titanium to functional Nitinol (NiTi). The discussion of this system revolves around the "Functionality vs. Processability" paradox. While the primary objective in standard dissimilar welding is structural strength, the success of an SS-NiTi joint is defined by its ability to undergo phase transformations after the welding cycle is complete.

As indicated in the Strengths section, the solid-state nature of FSW is the critical enabler for this coupling. By operating below the melting point, the process prevents the elemental volatilization—specifically the loss of Nickel—that frequently occurs in laser or arc welding. This preservation is vital because, as noted by Datta & Biswas [92], even a 0.1% shift in the Ni/Ti ratio can dramatically alter the transformation temperatures, potentially rendering the "smart" component useless for its intended thermal environment (the "Functional Drift" threat).

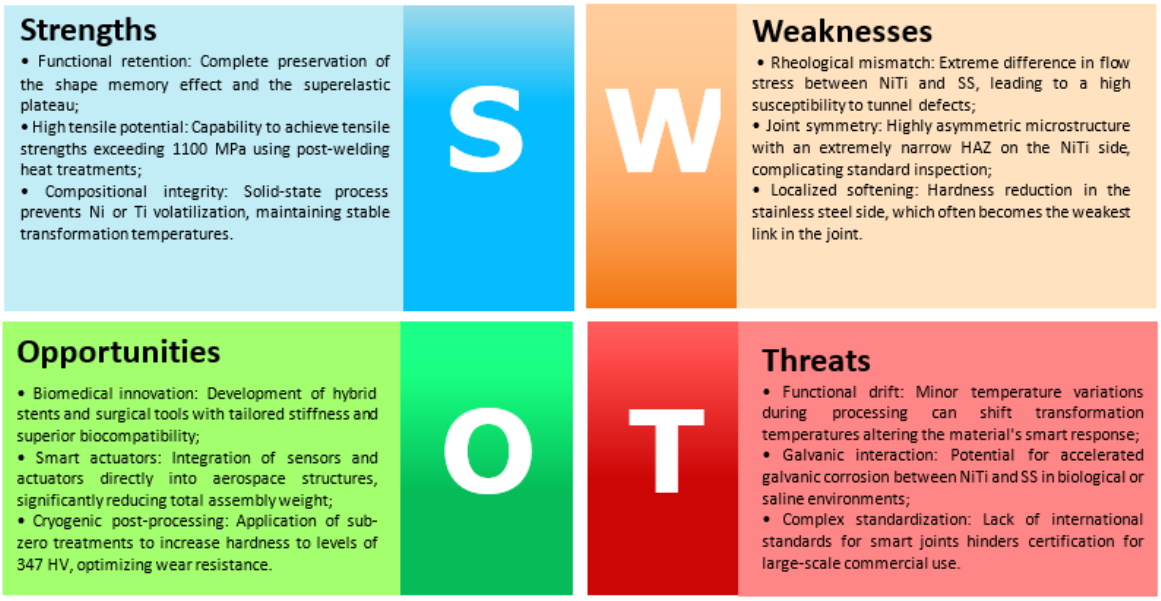

Figure 6. SWOT matrix for the dissimilar Friction Stir Welding of Stainless Steel and Nitinol (NiTi) alloys.

However, the analysis also reveals a significant Weakness in the form of rheological mismatch. Nitinol and Stainless Steel possess drastically different flow stresses and thermal conductivities. This disparity often results in an asymmetric material flow, which is the root cause of the tunnel defects observed in early trials. This physical incompatibility suggests that while the materials are chemically compatible (forming a stable interface), they are mechanically difficult to stir together.

The Opportunities identified, particularly in the Biomedical and Aerospace sectors, are contingent upon overcoming the joint's inherent asymmetry. The use of post-welding heat treatments (PWHT) and cryogenic processing, as explored by Shashikala [93], offers a strategic pathway to mitigate these weaknesses. By achieving a tensile strength of 1112 MPa, these treatments bridge the gap between the as-welded state and the high-performance requirements of actuators and stents.

Finally, the Threats section emphasizes a critical gap in current engineering: the lack of NDT (Non-Destructive Testing) standards for smart joints. Detecting whether the shape memory effect has been degraded inside a weld nugget is significantly more complex than identifying a simple crack. Therefore, the industrialization of SS-NiTi FSW will require not only process optimization but also the development of functional validation protocols to ensure that the superelastic plateau remains intact over the component's operational lifecycle.

4. Comparative Synthesis of Dissimilar FSW Systems

The comprehensive review and SWOT analyses conducted across the three dissimilar systems—Stainless Steel (SS) joined to Nickel (Ni), Titanium (Ti), and Nitinol (NiTi)—reveal a hierarchy of metallurgical complexity and industrial readiness. While FSW successfully addresses the "unweldability" typically associated with fusion processes, the strategic focus for each pair differs significantly.

4.1. Metallurgical Compatibility and Interfacial Kinetics

The SS-Ni system represents the highest level of metallurgical compatibility. As documented by Lemos et al. [76], the mutual solubility of Ni and Fe allows for a robust, ductile interface with minimal brittle phase formation. In this system, the discussion focuses on microstructural refinement (Hall-Petch strengthening) and the management of austenitic stability.

In contrast, the SS-Ti and SS-NiTi systems are governed by thermally activated interfacial kinetics, where the growth of the reaction layer follows a diffusion-controlled parabolic law. The primary challenge shifts from grain refinement to the strict suppression of brittle intermetallics (FeTi and Fe_2Ti). The research by Ishida et al. [86] and Li et al. [88] establishes a "critical threshold" of approximately 1 μm for the reaction layer in thin-gauge configurations (up to 3 mm) subjected to monotonic loading. Within this kinetic regime, the layer thickness is highly sensitive to the peak temperature and residence time (i.e., heat input); exceeding this limit facilitates a continuous brittle path that promotes interfacial cleavage, significantly compromising the joint's ductility and structural integrity regardless of the base metal's properties.

4.2. Functional vs. Structural Integrity

A critical distinction emerges when comparing Ti to NiTi:

- Structural Focus (SS-Ti): The objective is maximizing Ultimate Tensile Strength (UTS) and shear resistance for structural components in aerospace and power generation.
- Functional Focus (SS-NiTi): The objective is the preservation of the Shape Memory Effect (SME). As highlighted by Prabu et al. [91] and Datta & Biswas [92], the solid-state nature of FSW is not just a mechanical advantage but a functional necessity to prevent elemental volatilization. The success of the NiTi joint is measured by its superelastic plateau rather than just its breaking point.

4.3. The Role of Post-Processing and Thermal Management

Across all systems, the thermal dose (the combination of ω and *v*) is the decisive factor. However, the study by Shashikala et al. [93] introduces a vital strategic layer: Post-Welding Treatments.

The data suggests that:

(1) Thermal Management (during the process) prevents defects like "tunneling" caused by rheological mismatch.
(2) Post-Processing (Heat and Cryogenic treatments) is the key to unlocking the full potential of these joints, potentially elevating tensile strengths to over 1100 MPa in the case of Nitinol.

4.4. Strategic Viability (SWOT Synthesis)

The cross-system SWOT analysis reveals a clear industrial roadmap:

- SS-Ni: High viability for high-tenacity, corrosion-resistant offshore applications.
- SS-Ti: Technically challenging but highly rewarding for weight-sensitive aerospace structures, provided interfacial thickness is monitored.
- SS-NiTi: High-potential "smart" structures for biomedical and advanced robotics, requiring sophisticated monitoring to prevent functional drift.

4.5. Integrative Discussion: Metallurgical Integrity and Strategic Viability

The fundamental challenge in joining Stainless Steel to non-ferrous alloys like Titanium and Nitinol lies in the thermal management of the interface. As synthesized from the reviewed literature, FSW operates as a "double-edged sword". The frictional heat must be sufficient to achieve the plastic state required for material mixing, overcoming the significant rheological mismatch between the high-strength steel and the softer non-ferrous counterparts, yet low enough to inhibit the kinetics of brittle phase growth.

The transition from the SS-Ni system to the SS-Ti/NiTi systems highlights a shift in bonding mechanisms. In the former, the high mutual solubility allows for a relatively wide processing window. In the latter, however, the discussion is dominated by the diffusion-controlled growth of the reaction layer, governed by the parabolic law $X^2 = kt$, where the effective diffusion coefficient (D_{eff}) is significantly enhanced by pipe diffusion within the stir zone. The consensus among authors points to a 1 μm threshold; exceeding this limit triggers a transition from ductile to cleavage-dominated fracture, regardless of the refined grain structure achieved through dynamic recrystallization.

Crucial to this metallurgical evolution is the distinct nature of the Dynamic Recrystallization (DRX) occurring in the Stir Zone (SZ). In the austenitic stainless steel, the microstructure is refined via Discontinuous DRX (dDRX) characterized by grain boundary bulging. Conversely, the titanium alloys undergo Continuous DRX (cDRX) through sub-grain rotation, while the NiTi alloys exhibit a coupled mechanism between DRX and strain-induced martensitic transformation.

The reported 1 μm critical threshold for the Fe-Ti reaction layer must be interpreted within the context of thin-gauge butt-joint configurations (typically 1.5–3 mm). For these thicknesses, a reaction layer exceeding 1 μm generates a continuous brittle path that compromises joint ductility under monotonic tensile loading. Under conditions of fatigue or impact, or for thicker sections where the constraint effect differs, the critical thickness for maintaining structural integrity may be adjusted accordingly based on the specific stress-state.

A recurring theme in the dissimilar FSW of these alloys is the asymmetric material flow. Because the tool pin interacts with two materials of vastly different flow stresses and thermal conductivities, the "stirring" is never uniform. This is particularly evident in the SS-NiTi joints, where tunnel defects often appear along the weld line. This suggests that mechanical bonding is not merely a function of rotation speed but of the stacking sequence and tool offset.

By placing the harder material (Stainless Steel) on the advancing side or utilizing a tool offset toward the softer material, researchers have managed to optimize heat generation. This strategic positioning, however, introduces the threat of accelerated tool wear, creating a direct conflict between joint integrity and process cost-effectiveness.

Perhaps the most sophisticated aspect of this discussion is the preservation of smart functionality in NiTi alloys. The research by Prabu et al. [91] and Datta & Biswas [92] proves that FSW's solid-state nature is a superior alternative to fusion welding specifically because it maintains the Ni/Ti stoichiometry.

The "Functional Drift" identified in the SWOT analysis is a consequence of even minor thermal fluctuations that can shift the martensitic transformation temperatures. Therefore, the discussion moves beyond simple tensile strength (UTS) toward functional reliability. The ability to reach strengths over 1100 MPa via post-welding treatments, as shown by Shashikala et al. [93], suggests that the future of these hybrid joints lies in a multi-stage manufacturing approach: FSW for the initial bond, followed by thermal or cryogenic cycles to "tune" the final mechanical and functional properties.

5. Conclusions

This study investigated the capabilities of Friction Stir Welding (FSW) as a robust solution for joining stainless steel to various dissimilar non-ferrous alloys. Based on the comprehensive literature review and strategic analysis, the following conclusions can be drawn:

- Metallurgical Viability and Phase Control: FSW is highly effective in producing defect-free joints between stainless steel and alloys of Ni, Ti, and NiTi. The solid-state nature of the process is the decisive factor in suppressing massive intermetallic segregation and solidification cracking. However, for Ti-based systems, joint efficiency is strictly governed by the interfacial reaction layer, which must be maintained near a 1 μm threshold to prevent brittle cleavage.
- Functional Integrity of Smart Alloys: The joining of NiTi (Nitinol) to stainless steel successfully preserves the shape memory effect and superelasticity. This is attributed to the low-heat input of FSW, which prevents the volatilization of Nickel and maintains the critical Ni/Ti stoichiometry. While tunnel defects may arise from rheological mismatch, the functional "smart" response remains intact, a feat unattainable by conventional fusion welding. The shape memory effect is largely preserved, with representative studies indicating a shift in the Austenite finish temperature of less than 5 °C, ensuring that functional recovery remains within 90–95% of the base metal performance.
- Microstructural Refinement: In all analyzed systems, the stir zone (SZ) underwent intense dynamic recrystallization (DRX), resulting in significant grain refinement. This refinement leads to a localized increase in microhardness, reaching peaks such as 362 HV in Ti6321 joints.
- Mechanical Strength and Post-Processing: Although a slight reduction in ductility was noted due to the inherent brittleness of Fe-Ti and σ phases, the tensile strength of optimized joints can reach up to 88% of the base metal (CP-Ti) and exceed 1100 MPa (NiTi) when coupled with post-welding heat or cryogenic treatments. Optimized post-weld thermal cycles (typically solution treatment at ~800–900°C followed by water quenching) have demonstrated the ability to reach ultimate tensile strengths (UTS) exceeding 1100 MPa, as validated by standard ASTM E8 tensile testing across multiple representative specimens. This confirms that FSW joints are structurally viable for high-performance applications.
- Strategic Outlook: The SWOT analysis reveals that while SS-Ni joints are industrially mature for offshore use, SS-Ti and SS-NiTi joints represent the "high-performance" frontier. These systems require precise control over the thermal dose to balance material flow without triggering excessive intermetallic growth.

Despite the promising results, certain limitations remain. The rapid wear of FSW tools when processing high-strength alloys like SS 304 and Ti6Al4V increases operational costs. Furthermore, the detection of sub-micron intermetallic layers requires advanced characterization (EBSD/Micro-XRD) not always available in industrial settings. Future research should prioritize:

(1) Advanced Tooling: Implementation of PCBN (Polycrystalline Cubic Boron Nitride) or coated tungsten-carbide tools to extend service life.
(2) Thermal Management: Development of active cooling or stationary shoulder FSW to further restrict the growth of brittle phases.
(3) Long-term Durability: Investigation into the galvanic corrosion and fatigue-creep behavior of these hybrid interfaces, which is essential for certification in aerospace and biomedical sectors.

Recent advancements (2022–2024) suggest that hybrid processes, such as ultrasonic-assisted FSW and the use of Si_3N_4 ceramic tools, may further refine the IMC layers in SS/Ti joints, representing a key area for future research also.

The metallurgical strategies discussed herein have significant implications for high-performance industrial components. For instance, in the aerospace sector, the development of SS-Ti hybrid structures serves as a lightweight alternative to traditional fasteners and multi-part assemblies in engine turbine casings. In the biomedical field, the precise joining of NiTi-SS allows for the creation of smart surgical tools where the shape memory effect is localized at the tip.

Currently, these joints are often achieved via fusion welding with expensive interlayer foils or vacuum brazing, which are prone to elemental diffusion and excessive grain growth. Our analysis demonstrates that FSW acts as a superior technological substitute by replacing these indirect joining methods with a direct, solid-state thermomechanical bond. By controlling the heat input through the ω/v ratio, we bypass the need for filler materials, directly overcoming the embrittlement issues that legacy fusion-based methods fail to solve.

Author Contributions

N.P.V.S.: conceptualization, writing—original draft preparation, investigation; F.F.: methodology, supervision, writing—reviewing and editing; N.P.V.S., A.B. and G.P.: data curation, visualization; F.F., A.B. and G.P.: validation. All authors have read and agreed to the published version of the manuscript.

Funding

The work was developed under the "DRIVOLUTION—Transition to the factory of the future", Research Project Code 02/C05-i01.02/2022, Projet n.o 23, supported by European Structural and Investments Funds with the "Portugal2020" program scope.

Institutional Review Board Statement

Not applicable.

Informed Consent Statement

Not applicable.

Data Availability Statement

Not applicable.

Conflicts of Interest

The authors declare no conflict of interest.

Use of AI and AI-Assisted Technologies

No AI tools were utilized for this paper.

References

1. Bodukuri, A.K.; Eswaraiah, K.; Rajendar, K.; et al. Comparison of Aluminum Alloy 5083 Properties on TIGW and FSW Processes. *Mater. Today Proc.* **2017**, *4*, 10197–10201. https://doi.org/10.1016/j.matpr.2017.06.347.
2. Ahmed, M.M.Z.; Hajlaoui, K.; El-Sayed Seleman, M.M.; et al. Microstructure and Mechanical Properties of Friction Stir Welded 2205 Duplex Stainless Steel Butt Joints. *Materials* **2021**, *14*, 6640. https://doi.org/10.3390/ma14216640.
3. Habba, M.I.A.; Ahmed, M.M.Z. Friction Stir Welding-Based Technologies: A Comprehensive Review from the Sustainable Manufacturing Perspectives. *J. Mater. Res. Technol.* **2025**, *38*, 1–29. https://doi.org/10.1016/j.jmrt.2025.07.184.
4. Ragab, M.; Alsaleh, N.; El-Sayed Seleman, M.M.; et al. Weld Power, Heat Generation and Microstructure in FSW and SFSW of 11Cr-1.6W-1.6Ni Martensitic Stainless Steel: The Impact of Tool Rotation Rate. *Crystals* **2025**, *15*, 845. https://doi.org/10.3390/cryst15100845.
5. Feddal, I.; Chairi, M.; Di Bella, G. Analysis of Friction Stir Welding of Aluminum Alloys. *Metals* **2025**, *15*, 532. https://doi.org/10.3390/met15050532.
6. Singh, V.P.; Patel, S.K.; Ranjan, A.; et al. Recent Research Progress in Solid State Friction-Stir Welding of Aluminium–Magnesium Alloys: A Critical Review. *J. Mater. Res. Technol.* **2020**, *9*, 6217–6256. https://doi.org/10.1016/j.jmrt.2020.01.008.
7. Ahmed, M.M.Z.; El-Sayed Seleman, M.M.; Fydrych, D.; et al. Review on Friction Stir Welding of Dissimilar Magnesium and Aluminum Alloys: Scientometric Analysis and Strategies for Achieving High-Quality Joints. *J. Magnes. Alloys* **2023**, *11*, 4082–4127. https://doi.org/10.1016/j.jma.2023.09.039.

8. Radu, B.; Hulka, I.; Cojocaru, R.; et al. Microstructural Transformation during Dissimilar Friction Stir Welding (FSW) of Aluminum-Cooper Alloys. *Solid State Phenom.* **2016**, *254*, 65–70. https://doi.org/10.4028/www.scientific.net/SSP.254.65.
9. Gangwar, K.; Ramulu, M. Friction Stir Welding of Titanium Alloys: A Review. *Mater. Des.* **2018**, *141*, 230–255. https://doi.org/10.1016/j.matdes.2017.12.033.
10. Siddiquee, A.N.; Pandey, S. Experimental Investigation on Deformation and Wear of WC Tool during Friction Stir Welding (FSW) of Stainless Steel. *Int. J. Adv. Manuf. Technol.* **2014**, *73*, 479–486. https://doi.org/10.1007/s00170-014-5846-z.
11. Mironov, S.; Sato, Y.S.; Kokawa, H.; et al. Structural Response of Superaustenitic Stainless Steel to Friction Stir Welding. *Acta Mater.* **2011**, *59*, 5472–5481. https://doi.org/10.1016/j.actamat.2011.05.021.
12. Mubiayi, M.P. Current Developments in Friction Stir Welding (FSW) and Friction Stir Spot Welding (FSSW) of Aluminium and Titanium Alloys. In Proceedings of the 4th International Electronic Conference on Applied Sciences, online, 27 October–10 November 2023; p. 184. https://doi.org/10.3390/ASEC2023-15881.
13. Patel, M.M.; Badheka, V.J. A Review on Friction Stir Welding (FSW) Process for Dissimilar Aluminium to Steel Metal Systems. *Weld. Int.* **2024**, *38*, 91–115. https://doi.org/10.1080/09507116.2023.2291064.
14. Jafarzadegan, M.; Feng, A.H.; Abdollah-zadeh, A.; et al. Microstructural Characterization in Dissimilar Friction Stir Welding between 304 Stainless Steel and St37 Steel. *Mater. Charact.* **2012**, *74*, 28–41. https://doi.org/10.1016/j.matchar.2012.09.004.
15. Li, H.B.; Jiang, Z.H.; Feng, H.; et al. Microstructure, Mechanical and Corrosion Properties of Friction Stir Welded High Nitrogen Nickel-Free Austenitic Stainless Steel. *Mater. Des.* **2015**, *84*, 291–299. https://doi.org/10.1016/j.matdes.2015.06.103.
16. Mishra, R.S.; Ma, Z.Y. Friction Stir Welding and Processing. *Mater. Sci. Eng. R* **2005**, *50*, 1–78. https://doi.org/10.1016/j.mser.2005.07.001.
17. Taheri, H.; Kilpatrick, M.; Norvalls, M.; et al. Investigation of Nondestructive Testing Methods for Friction Stir Welding. *Metals* **2019**, *9*, 624. https://doi.org/10.3390/met9060624.
18. Meyghani, B.; Awang, M.; Emamian, S.S.; et al. A Comparison of Different Finite Element Methods in the Thermal Analysis of Friction Stir Welding (FSW). *Metals* **2017**, *7*, 450. https://doi.org/10.3390/met7100450.
19. Murr, L.E. A Review of FSW Research on Dissimilar Metal and Alloy Systems. *J. Mater. Eng. Perform.* **2010**, *19*, 1071–1089. https://doi.org/10.1007/s11665-010-9598-0.
20. Singh, A.; Sharma, S.K.; Batish, A. Dynamic Recrystallization during Solid State Friction Stir Welding/Processing/Additive Manufacturing: Mechanisms, Microstructure Evolution, Characterization, Modeling Techniques and Challenges. *Crit. Rev. Solid State Mater. Sci.* **2025**, *50*, 77–135. https://doi.org/10.1080/10408436.2024.2391333.
21. Fraser, K.; St-Georges, L.; Kiss, L.I. A Mesh-Free Solid-Mechanics Approach for Simulating the Friction Stir-Welding Process. In *Joining Technologies*; InTech: London, UK, 2016. https://doi.org/10.5772/64159.
22. Malik, V.; Sanjeev, N.K.; Hebbar, H.S.; et al. Time Efficient Simulations of Plunge and Dwell Phase of FSW and Its Significance in FSSW. *Procedia Mater. Sci.* **2014**, *5*, 630–639. https://doi.org/10.1016/j.mspro.2014.07.309.
23. Shi, L.; Wu, C.S. Transient Model of Heat Transfer and Material Flow at Different Stages of Friction Stir Welding Process. *J. Manuf. Process.* **2017**, *25*, 323–339. https://doi.org/10.1016/j.jmapro.2016.11.008.
24. Lu, X.; Qiao, J.; Qian, J.; et al. Welding Parameters Optimization during Plunging and Dwelling Phase of FSW 2219 Aluminum Alloy Thick Plate. *Int. J. Adv. Manuf. Technol.* **2022**, *120*, 6163–6173. https://doi.org/10.1007/s00170-022-09098-z.
25. Guerdoux, S.; Fourment, L. A 3D Numerical Simulation of Different Phases of Friction Stir Welding. *Model. Simul. Mater. Sci. Eng.* **2009**, *17*, 075001. https://doi.org/10.1088/0965-0393/17/7/075001.
26. Liu, F.C.; Hovanski, Y.; Miles, M.P.; et al. A Review of Friction Stir Welding of Steels: Tool, Material Flow, Microstructure, and Properties. *J. Mater. Sci. Technol.* **2018**, *34*, 39–57. https://doi.org/10.1016/j.jmst.2017.10.024.
27. Abbasi Gharacheh, M.; Kokabi, A.H.; Daneshi, G.H.; et al. The Influence of the Ratio of 'Rotational Speed/Traverse Speed' (ω/v) on Mechanical Properties of AZ31 Friction Stir Welds. *Int. J. Mach. Tools Manuf.* **2006**, *46*, 1983–1987. https://doi.org/10.1016/j.ijmachtools.2006.01.007.
28. Mohammadi, J.; Behnamian, Y.; Mostafaei, A.; et al. Tool Geometry, Rotation and Travel Speeds Effects on the Properties of Dissimilar Magnesium/Aluminum Friction Stir Welded Lap Joints. *Mater. Des.* **2015**, *75*, 95–112. https://doi.org/10.1016/j.matdes.2015.03.017.
29. Su, H.; Wu, C.S.; Pittner, A.; et al. Simultaneous Measurement of Tool Torque, Traverse Force and Axial Force in Friction Stir Welding. *J. Manuf. Process.* **2013**, *15*, 495–500. https://doi.org/10.1016/j.jmapro.2013.09.001.
30. Mugada, K.K.; Adepu, K. Influence of Tool Shoulder End Features on Friction Stir Weld Characteristics of Al-Mg-Si Alloy. *Int. J. Adv. Manuf. Technol.* **2018**, *99*, 1553–1566. https://doi.org/10.1007/s00170-018-2602-9.
31. da Silva, Y.C.; Oliveira Júnior, F.J.V.; dos Santos, J.F.; et al. Numerical Investigation of the Influence of FSW Parameters on the Heat and Mass Transfer of Austenitic Stainless Steels. *Weld. World* **2020**, *64*, 2019–2032. https://doi.org/10.1007/s40194-020-00980-6.
32. Quan, G.-Z.; Li, G.-S.; Chen, T.; et al. Dynamic Recrystallization Kinetics of 42CrMo Steel during Compression at Different Temperatures and Strain Rates. *Mater. Sci. Eng. A* **2011**, *528*, 4643–4651. https://doi.org/10.1016/j.msea.2011.02.090.

33. Kangazian, J.; Shamanian, M. Microstructure and Mechanical Characterization of Incoloy 825 Ni-Based Alloy Welded to 2507 Super Duplex Stainless Steel through Dissimilar Friction Stir Welding. *Trans. Nonferrous Met. Soc. China* **2019**, *29*, 1677–1688. https://doi.org/10.1016/S1003-6326(19)65074-0.
34. Huang, Y.; Meng, X.; Xie, Y.; et al. Friction Stir Welding/Processing of Polymers and Polymer Matrix Composites. *Compos. Part A Appl. Sci. Manuf.* **2018**, *105*, 235–257. https://doi.org/10.1016/j.compositesa.2017.12.005.
35. Song, K.H.; Fujii, H.; Nakata, K. Effect of Welding Speed on Microstructural and Mechanical Properties of Friction Stir Welded Inconel 600. *Mater. Des.* **2009**, *30*, 3972–3978. https://doi.org/10.1016/j.matdes.2009.05.033.
36. Mishra, R.S.; De, P.S.; Kumar, N. Fundamental Physical Metallurgy Background for FSW/P. In *Friction Stir Welding and Processing*; Springer: Cham, Switzerland, 2014; pp. 59–93. https://doi.org/10.1007/978-3-319-07043-8_3.
37. Azeez, S.; Akinlabi, E. Sustainability of Manufacturing Technology: Friction Stir Welding in Focus. *Prog. Ind. Ecol.* **2018**, *12*, 419–438. https://doi.org/10.1504/PIE.2018.097188.
38. Al-Sabur, R.; Serier, M. Material Sustainability During Friction Stir Joining. In *Sustainable Machining and Green Manufacturing*; Wiley: Hoboken, NJ, USA, 2024; pp. 131–153. https://doi.org/10.1002/9781394197866.ch7.
39. Majeed, T.; Wahid, M.A.; Alam, M.N.; et al. Friction Stir Welding: A Sustainable Manufacturing Process. *Mater. Today Proc.* **2021**, *46*, 6558–6563. https://doi.org/10.1016/j.matpr.2021.04.025.
40. Abbasi, M.; Bagheri, B.; Abdollahzadeh, A.; et al. A Different Attempt to Improve the Formability of Aluminum Tailor Welded Blanks (TWB) Produced by the FSW. *Int. J. Mater. Form.* **2021**, *14*, 1189–1208. https://doi.org/10.1007/s12289-021-01632-w.
41. Verma, M.; Ahmed, S.; Saha, P. Challenges, Process Requisites/Inputs, Mechanics and Weld Performance of Dissimilar Micro-Friction Stir Welding (Dissimilar μFSW): A Comprehensive Review. *J. Manuf. Process.* **2021**, *68*, 249–276. https://doi.org/10.1016/j.jmapro.2021.05.045.
42. Debbarma, P.P.; Das, B. State-of-the-Art Survey of Literature for Finding an Effective Solution to Mitigate the Exit-Hole Defect in Friction Stir Welded Samples. *Proc. Inst. Mech. Eng. Part E J. Process Mech. Eng.* **2024**, *240*, 1145–1160. https://doi.org/10.1177/09544089241228946.
43. Dialami, N.; Chiumenti, M.; Cervera, M.; et al. Challenges in Thermo-Mechanical Analysis of Friction Stir Welding Processes. *Arch. Comput. Methods Eng.* **2017**, *24*, 189–225. https://doi.org/10.1007/s11831-015-9163-y.
44. Lunetto, V.; Maddis, M.; Lombardi, F.; et al. A Review of Friction Stir Welding of Industrial Alloys: Tool Design and Process Parameters. *J. Manuf. Mater. Process.* **2025**, *9*, 36. https://doi.org/10.3390/jmmp9020036.
45. Muralimohan, C.H.; Muthupandi, V.; Sivaprasad, K. Properties of Friction Welding Titanium-Stainless Steel Joints with a Nickel Interlayer. *Procedia Mater. Sci.* **2014**, *5*, 1120–1129. https://doi.org/10.1016/j.mspro.2014.07.406.
46. Sanders, D.G.; Edwards, P.; Cantrell, A.M.; et al. Friction Stir-Welded Titanium Alloy Ti-6Al-4V: Microstructure, Mechanical and Fracture Properties. *JOM* **2015**, *67*, 1054–1063. https://doi.org/10.1007/s11837-015-1376-x.
47. Rodriguez, J.; Ramirez, A.J. Friction Stir Welding of Mild Steel to Alloy 625—Development of Welding Parameters. *Sci. Technol. Weld. Join.* **2014**, *19*, 343–349. https://doi.org/10.1179/1362171814Y.0000000198.
48. Salih, O.S.; Ou, H.; Sun, W.; et al. A Review of Friction Stir Welding of Aluminium Matrix Composites. *Mater. Des.* **2015**, *86*, 61–71. https://doi.org/10.1016/j.matdes.2015.07.071.
49. Singh, K.; Singh, G.; Singh, H. Review on Friction Stir Welding of Magnesium Alloys. *J. Magnes. Alloys* **2018**, *6*, 399–416. https://doi.org/10.1016/j.jma.2018.06.001.
50. Singh, R.P.; Dubey, S.; Singh, A.; et al. A Review Paper on Friction Stir Welding Process. *Mater. Today Proc.* **2021**, *38*, 6–11. https://doi.org/10.1016/j.matpr.2020.05.208.
51. Sen, M.; Ozcan, M.E.; Yildiz, Y.O.; et al. A Comprehensive Study on Friction Stir Welding: A Review. *Soldag. Inspeção* **2025**, *30*, e3016. https://doi.org/10.1590/0104-9224/si30.16.
52. Santhakumari, A.; Senthilkumar, T.; Mahadevan, G.; et al. Interface and Microstructural Characteristics of Titanium and 304 Stainless Steel Dissimilar Joints by Upset Butt Welding Using a Gleeble Thermo Mechanical Simulator. *J. Mater. Res. Technol.* **2023**, *26*, 7460–7470. https://doi.org/10.1016/j.jmrt.2023.09.098.
53. Tanmay; Alam, Z.; Panda, S.S. A Review on Joining of Dissimilar Metals with Highly Differential Thermomechanical Properties. *J. Mater. Eng. Perform.* **2025**, *34*, 8219–8231. https://doi.org/10.1007/s11665-024-10279-y.
54. Mukherjee, T.; DebRoy, T. Control of Asymmetric Track Geometry in Printed Parts of Stainless Steels, Nickel, Titanium and Aluminum Alloys. *Comput. Mater. Sci.* **2020**, *182*, 109791. https://doi.org/10.1016/j.commatsci.2020.109791.
55. Kah, P.; Shrestha, M.; Martikainen, J. Trends in Joining Dissimilar Metals by Welding. *Appl. Mech. Mater.* **2013**, *440*, 269–276. https://doi.org/10.4028/www.scientific.net/AMM.440.269.
56. Giudice, F.; Missori, S.; Scolaro, C.; et al. A Review on Fusion Welding of Dissimilar Ferritic/Austenitic Steels: Processing and Weld Zone Metallurgy. *J. Manuf. Mater. Process.* **2024**, *8*, 96. https://doi.org/10.3390/jmmp8030096.
57. Xue, P.; Xiao, B.L.; Ma, Z.Y. Effect of Interfacial Microstructure Evolution on Mechanical Properties and Fracture Behavior of Friction Stir-Welded Al-Cu Joints. *Metall. Mater. Trans. A* **2015**, *46*, 3091–3103. https://doi.org/10.1007/s11661-015-2909-1.

58. Sahu, M.; Paul, A.; Ganguly, S. Formation of Mechanical Property Gradient along the Sheet Thickness Due to the Patterned Fe/Al IMC Layers in the Interface in Dissimilar FSW of HSLA Steel to AA 5083. *Mater. Charact.* **2023**, *203*, 113146. https://doi.org/10.1016/j.matchar.2023.113146.
59. Beygi, R.; Carbas, R.J.C.; Marques, E.A.S.; et al. Mechanism of Toughness Enhancement of Brittle Fracture by Intermittent η-Intermetallic in Al/Cu Joint Made by FSW. *Mater. Sci. Eng. A* **2024**, *890*, 145907. https://doi.org/10.1016/j.msea.2023.145907.
60. Krauss, G. *Steels: Processing, Structure, and Performance, Second Edition*; ASM International: Materials Park, OH, USA, 2015. https://doi.org/10.31399/asm.tb.spsp2.9781627082655.
61. Al Minnath, M. Metals and Alloys for Biomedical Applications. In *Fundamental Biomaterials: Metals*; Elsevier: Amsterdam, The Netherlands, 2018; pp. 167–174. https://doi.org/10.1016/B978-0-08-102205-4.00007-6.
62. Hanawa, T. Overview of Metals and Applications. In *Metals for Biomedical Devices*; Elsevier: Amsterdam, The Netherlands, 2010; pp. 3–24. https://doi.org/10.1533/9781845699246.1.3.
63. Tahchieva, A.B.; Llorca-Isern, N.; Cabrera, J.-M. Duplex and Superduplex Stainless Steels: Microstructure and Property Evolution by Surface Modification Processes. *Metals* **2019**, *9*, 347. https://doi.org/10.3390/met9030347.
64. Zhang, Y.; Wu, S.; Cheng, F. A Specially-Designed Super Duplex Stainless Steel with Balanced Ferrite: Austenite Ratio Fabricated via Flux-Cored Wire Arc Additive Manufacturing: Microstructure Evolution, Mechanical Properties and Corrosion Resistance. *Mater. Sci. Eng. A* **2022**, *854*, 143809. https://doi.org/10.1016/j.msea.2022.143809.
65. Mathers, G. Material Standards, Designations and Alloys. In *The Welding of Aluminium and Its Alloys*; Elsevier: Amsterdam, The Netherlands, 2002; pp. 35–50. https://doi.org/10.1533/9781855737631.35.
66. Liu, S.; Liang, L. Research Progress on Alloying of High Chromium Cast Iron—Austenite Stabilizing Elements and Modifying Elements. *Crystals* **2025**, *15*, 210. https://doi.org/10.3390/cryst15030210.
67. Francis, R.; Byrne, G. Duplex Stainless Steels—Alloys for the 21st Century. *Metals* **2021**, *11*, 836. https://doi.org/10.3390/met11050836.
68. Saeid, T.; Abdollah-zadeh, A.; Shibayanagi, T.; et al. On the Formation of Grain Structure during Friction Stir Welding of Duplex Stainless Steel. *Mater. Sci. Eng. A* **2010**, *527*, 6484–6488. https://doi.org/10.1016/j.msea.2010.07.011.
69. Najafizadeh, M.; Yazdi, S.; Bozorg, M.; et al. Classification and Applications of Titanium and Its Alloys: A Review. *J. Alloys Compd. Commun.* **2024**, *3*, 100019. https://doi.org/10.1016/j.jacomc.2024.100019.
70. Ezugwu, E.O.; Batista Da Silva, R.; Falco Sales, W.; et al. Overview of the Machining of Titanium Alloys. In *Encyclopedia of Sustainable Technologies*; Elsevier: Amsterdam, The Netherlands, 2017; pp. 487–506. https://doi.org/10.1016/B978-0-12-409548-9.10216-7.
71. Gao, K.; Zhang, Y.; Yi, J.; et al. Overview of Surface Modification Techniques for Titanium Alloys in Modern Material Science: A Comprehensive Analysis. *Coatings* **2024**, *14*, 148. https://doi.org/10.3390/coatings14010148.
72. Semiatin, S.L. An Overview of the Thermomechanical Processing of α/β Titanium Alloys: Current Status and Future Research Opportunities. *Metall. Mater. Trans. A* **2020**, *51*, 2593–2625. https://doi.org/10.1007/s11661-020-05625-3.
73. Yonezawa, T. Nickel Alloys: Properties and Characteristics. In *Comprehensive Nuclear Materials*; Elsevier: Amsterdam, The Netherlands, 2012; pp. 233–266. https://doi.org/10.1016/B978-0-08-056033-5.00016-1.
74. Weber, J.H.; Fahrman, M.G.; Crum, J.R. Nickel: Alloying. In *Encyclopedia of Materials: Science and Technology*; Elsevier: Amsterdam, The Netherlands, 2001; pp. 6135–6140. https://doi.org/10.1016/B0-08-043152-6/01085-8.
75. Das, N. Advances in Nickel-Based Cast Superalloys. *Trans. Indian Inst. Met.* **2010**, *63*, 265–274. https://doi.org/10.1007/s12666-010-0036-7.
76. Lemos, G.V.B.; Hanke, S.; Dos Santos, J.F.; et al. Progress in Friction Stir Welding of Ni Alloys. *Sci. Technol. Weld. Join.* **2017**, *22*, 643–657. https://doi.org/10.1080/13621718.2017.1288953.
77. Srivastava, A.K.; Sharma, A. Advances in Joining and Welding Technologies for Automotive and Electronic Applications. *Am. J. Mater. Eng. Technol.* **2017**, *5*, 7–13. https://doi.org/10.12691/materials-5-1-2.
78. Song, K.H.; Nakata, K. Effect of Precipitation on Post-Heat-Treated Inconel 625 Alloy after Friction Stir Welding. *Mater. Des.* **2010**, *31*, 2942–2947. https://doi.org/10.1016/j.matdes.2009.12.020.
79. Saeid, T.; Abdollah-zadeh, A.; Assadi, H.; et al. Effect of Friction Stir Welding Speed on the Microstructure and Mechanical Properties of a Duplex Stainless Steel. *Mater. Sci. Eng. A* **2008**, *496*, 262–268. https://doi.org/10.1016/j.msea.2008.05.025.
80. Thomas, W.M.; Johnson, K.I.; Wiesner, C.S. Friction Stir Welding—Recent Developments in Tool and Process Technologies. *Adv. Eng. Mater.* **2003**, *5*, 485–490. https://doi.org/10.1002/adem.200300355.
81. Mondal, M.; Das, H.; Ahn, E.Y.; et al. Characterization of Friction Stir Welded Joint of Low Nickel Austenitic Stainless Steel and Modified Ferritic Stainless Steel. *Met. Mater. Int.* **2017**, *23*, 948–957. https://doi.org/10.1007/s12540-017-6845-z.
82. Casanova, J.; Sorger, G.; Vilaça, P.; et al. Microstructure and Mechanical Properties of 9% Nickel Steel Welded by FSW. *Int. J. Adv. Manuf. Technol.* **2020**, *111*, 3225–3240. https://doi.org/10.1007/s00170-020-06313-7.
83. Thomas, W.M.; Threadgill, P.L.; Nicholas, E.D. Feasibility of Friction Stir Welding Steel. *Sci. Technol. Weld. Join.* **1999**, *4*, 365–372. https://doi.org/10.1179/136217199101538012.

84. Threadgill, P.L.; Leonard, A.J.; Shercliff, H.R.; et al. Friction Stir Welding of Aluminium Alloys. *Int. Mater. Rev.* **2009**, *54*, 49–93.
85. Fazel-Najafabadi, M.; Kashani-Bozorg, S.F.; Zarei-Hanzaki, A. Joining of CP-Ti to 304 Stainless Steel Using Friction Stir Welding Technique. *Mater. Des.* **2010**, *31*, 4800–4807. https://doi.org/10.1016/j.matdes.2010.05.003.
86. Ishida, K.; Gao, Y.; Nagatsuka, K.; et al. Microstructures and Mechanical Properties of Friction Stir Welded Lap Joints of Commercially Pure Titanium and 304 Stainless Steel. *J. Alloys Compd.* **2015**, *630*, 172–177. https://doi.org/10.1016/j.jallcom.2015.01.004.
87. Gotawala, N.; Shrivastava, A. Microstructural Analysis and Mechanical Behavior of SS 304 and Titanium Joint from Friction Stir Butt Welding. *Mater. Sci. Eng. A* **2020**, *789*, 139658. https://doi.org/10.1016/j.msea.2020.139658.
88. Li, S.; Chen, Y.; Kang, J.; et al. Interfacial Microstructures and Mechanical Properties of Dissimilar Titanium Alloy and Steel Friction Stir Butt-Welds. *J. Manuf. Process.* **2019**, *40*, 160–168. https://doi.org/10.1016/j.jmapro.2019.03.015.
89. West, P.; Shunmugasamy, V.C.; Usman, C.A.; et al. Part II.: Dissimilar Friction Stir Welding of Nickel Titanium Shape Memory Alloy to Stainless Steel—Microstructure, Mechanical and Corrosion Behavior. *J. Adv. Join. Process.* **2021**, *4*, 100072. https://doi.org/10.1016/j.jajp.2021.100072.
90. Zhi-hong, F.; Di-qiu, H.; Hong, W. Friction Stir Welding of Aluminum Alloys. *J. Wuhan Univ. Technol.-Mater. Sci. Ed.* **2004**, *19*, 61–64. https://doi.org/10.1007/BF02838366.
91. Prabu, S.S.M.; Madhu, H.C.; Perugu, C.S.; et al. Shape Memory Effect, Temperature Distribution and Mechanical Properties of Friction Stir Welded Nitinol. *J. Alloys Compd.* **2019**, *776*, 334–345. https://doi.org/10.1016/j.jallcom.2018.10.200.
92. Datta, S.; Biswas, P. A Review on Present Status of Friction Stir Welding of Nitinol, a Functionally Advanced, Versatile and Widely Used Shape Memory Alloy. In *Shape Memory Alloys—New Advances*; IntechOpen: London, UK, 2023. https://doi.org/10.5772/intechopen.1003677.
93. Shashikala, A.; Muniraju, M.; Pakkirappa, H. Experimental Investigation of Rotary Friction Welding on the Mechanical Properties of NiTinol Alloy. *Weld. Int.* **2023**, *37*, 163–173. https://doi.org/10.1080/09507116.2023.2202343.